NASA/TM—2004-213093

Far-Field Acoustic Characteristics of Multiple Blade-Vane Configurations for a High Tip Speed Fan

Richard P. Woodward
Glenn Research Center, Cleveland, Ohio

John A. Gazzaniga
QSS Group, Inc., Cleveland, Ohio

Christopher E. Hughes
Glenn Research Center, Cleveland, Ohio

May 2004

The NASA STI Program Office . . . in Profile

Since its founding, NASA has been dedicated to the advancement of aeronautics and space science. The NASA Scientific and Technical Information (STI) Program Office plays a key part in helping NASA maintain this important role.

The NASA STI Program Office is operated by Langley Research Center, the Lead Center for NASA's scientific and technical information. The NASA STI Program Office provides access to the NASA STI Database, the largest collection of aeronautical and space science STI in the world. The Program Office is also NASA's institutional mechanism for disseminating the results of its research and development activities. These results are published by NASA in the NASA STI Report Series, which includes the following report types:

- TECHNICAL PUBLICATION. Reports of completed research or a major significant phase of research that present the results of NASA programs and include extensive data or theoretical analysis. Includes compilations of significant scientific and technical data and information deemed to be of continuing reference value. NASA's counterpart of peer-reviewed formal professional papers but has less stringent limitations on manuscript length and extent of graphic presentations.

- TECHNICAL MEMORANDUM. Scientific and technical findings that are preliminary or of specialized interest, e.g., quick release reports, working papers, and bibliographies that contain minimal annotation. Does not contain extensive analysis.

- CONTRACTOR REPORT. Scientific and technical findings by NASA-sponsored contractors and grantees.

- CONFERENCE PUBLICATION. Collected papers from scientific and technical conferences, symposia, seminars, or other meetings sponsored or cosponsored by NASA.

- SPECIAL PUBLICATION. Scientific, technical, or historical information from NASA programs, projects, and missions, often concerned with subjects having substantial public interest.

- TECHNICAL TRANSLATION. English-language translations of foreign scientific and technical material pertinent to NASA's mission.

Specialized services that complement the STI Program Office's diverse offerings include creating custom thesauri, building customized databases, organizing and publishing research results . . . even providing videos.

For more information about the NASA STI Program Office, see the following:

- Access the NASA STI Program Home Page at ***http://www.sti.nasa.gov***

- E-mail your question via the Internet to help@sti.nasa.gov

- Fax your question to the NASA Access Help Desk at 301–621–0134

- Telephone the NASA Access Help Desk at 301–621–0390

- Write to:
  NASA Access Help Desk
  NASA Center for AeroSpace Information
  7121 Standard Drive
  Hanover, MD 21076

NASA/TM—2004-213093

Far-Field Acoustic Characteristics of Multiple Blade-Vane Configurations for a High Tip Speed Fan

Richard P. Woodward
Glenn Research Center, Cleveland, Ohio

John A. Gazzaniga
QSS Group, Inc., Cleveland, Ohio

Christopher E. Hughes
Glenn Research Center, Cleveland, Ohio

National Aeronautics and
Space Administration

Glenn Research Center

May 2004

A supplemental CD is included in the back of this report. It contains far-field SPL results for each configuration, EPNL and PWL table, daily acoustic logs, descriptive tables for tests parameters, and technical reports pertaining to the subject fan test. For a complete listing see the file named *CD Contents.pdf* on the supplemental CD.

Available from

NASA Center for Aerospace Information
7121 Standard Drive
Hanover, MD 21076

National Technical Information Service
5285 Port Royal Road
Springfield, VA 22100

Available electronically at http://gltrs.grc.nasa.gov

Far-Field Acoustic Characteristics of Multiple Blade-Vane Configurations for a High Tip Speed Fan

Richard P. Woodward
National Aeronautics and Space Administration
Glenn Research Center
Cleveland, Ohio 44135

John A. Gazzaniga
QSS Group, Inc.
Cleveland, Ohio 44135

Christopher E. Hughes
National Aeronautics and Space Administration
Glenn Research Center
Cleveland, Ohio 44135

Summary

The acoustic characteristics of a model high-speed fan stage were measured in the NASA Glenn 9- by 15-Foot Low Speed Wind Tunnel (LSWT) at takeoff and approach flight conditions. The fan was designed for a corrected rotor tip speed of 442 m/s (1450 ft/s), and had a powered core, or booster stage, giving the model a nominal bypass ratio of 5. A simulated engine pylon and nozzle bifurcation was contained within the bypass duct. The fan stage consisted of all combinations of 3 possible rotors, and 3 stator vane sets. The 3 rotors were (1) wide chord, (2) forward swept, and (3) shrouded. The 3 stator sets were (1) baseline, moderately swept, (2) swept and leaned, and (3) swept integral vane/frame which incorporated some of the swept and leaned features as well as eliminated the downstream support structure. The baseline configuration is considered to be the wide chord rotor with the radial vane stator. A flyover Effective Perceived Noise Level (EPNL) code was used to generate relative EPNL values for the various configurations. The swept and leaned stator showed a 3 EPNdB reduction at lower fan speeds relative to the baseline stator; while the swept integral vane/frame stator showed lowest noise levels at high fan speeds. The baseline, wide chord rotor was typically the quietest of the three rotors. A tone removal study was performed to assess the acoustic benefits of removing the fundamental rotor interaction tone and its harmonics. Reprocessing the acoustic results with the bypass tone removed had the most impact on reducing fan noise at transonic rotor speeds. Removal of the bypass rotor interaction tones (BPF and nBPF) showed up to a 6 EPNdB noise reduction at transonic rotor speeds relative to noise levels for the baseline (wide chord rotor and radial stator; all tones present) configuration.

Introduction

A major mechanism of aircraft engine noise comes from interaction of the rotor viscous wake with the exit guide vanes, or stators. The most prominent component of this interaction noise is tones at multiples of the rotor blade passage frequency, although there also exists a broadband component of this rotor-stator noise. Traditional methods of reducing this interaction noise have been to select blade to vane ratios to satisfy the cutoff criterion for propagation of the fundamental rotor tone (ref. 1) and increased

axial spacing between the rotor and stator (ref. 2). Increased rotor-stator axial spacing may somewhat degrade the fan aerodynamic performance and increase the overall engine weight.

Stator vane lean and/or sweep have been suggested as a mechanism to reduce the severity of the rotor wake interaction with the stator vane. Vane sweep is the axial displacement of the vane with radius such that the tip region is further downstream than the hub. Stator lean is the circumferential displacement of the vane stacking line relative to the radial direction. Both of these stator modifications have been previously investigated as a means to reduce the stator response to the rotor downwash, thereby reducing the rotor-stator acoustic response. Kazin (ref. 3) demonstrated rotor-stator interaction reductions in the 2BPF tone from 1.5 to 3.5 dB0 associated with a stator leaned 30° in the direction of fan rotation.

Analytical studies (ref. 4.) have suggested that both stator lean and sweep, if properly applied, may significantly reduce rotor-stator interaction tone noise. Optimal stator lean and sweep offers the possibility of reducing the overall engine weight through decreased axial rotor-stator spacing or achieving additional tone noise reduction for a particular rotor-stator spacing.

The results of ref. 5 showed that stator sweep and lean could give a 3 EPNdB noise reduction for a lower design tip speed (305 m/s (1000 ft/s)) fan. Thus, it was desirable to explore the acoustic benefits of stator sweep and lean for a higher design tip speed fan. Rotor forward sweep has the potential of reducing multiple pure tone generation at transonic and higher rotor speeds through reduction of the relative velocity normal to the blade leading edge, thereby reducing the magnitude of the leading edge shock and consequent MPT generation. Additionally, a forward swept rotor may have increased rotor-stator spacing toward the tip region, which could reduce the severity of the rotor wake upon the stator. Initial acoustic results for the subject (high design rotor speed) research fan with the baseline wide chord rotor and three stator sets (ref. 6) verified that similar acoustic benefits of stator sweep and lean could be achieved at subsonic rotor tip speeds.

This paper presents comprehensive acoustic results for an advanced high tip speed model fan that was tested in 1999 in the NASA Glenn 9- by 15-Foot LSWT. The 9- by 15-Foot LSWT provides an anechoic testing environment at representative takeoff and approach flight speeds. The model was representative of what is currently used on a 5 to 6 bypass ratio, 442 m/s (1450 ft/s) rotor tip speed turbofan. The research fan stage consisted of all combinations of 3 possible rotors, and 3 stator vane sets. The 3 rotors were (1) wide chord, (2) forward swept, and (3) shrouded. The 3 stator sets were (1) baseline, moderately swept, (2) swept and leaned, and (3) swept integral vane/frame which incorporated some of the swept and leaned features as well as eliminated the downstream support structure.

Description of Fan Test

Research Fan

The high-speed fan model was designed and built by General Electric Aircraft Engines under contract to NASA Glenn Research Center (Contract NAS3–7720). Figure 1 is a photograph of the model fan installed in the NASA Glenn 9- by 15-Foot LSWT. The fan was tested at a free stream Mach number of 0.10 in the test section, which is sufficient to achieve acoustic flight effect (ref. 7) and provides acoustic data representative of takeoff/approach operation. All data were taken at 0° fan axis angle of attack.

The NASA Glenn Ultra High Bypass (UHB) drive rig (ref. 8) was used to power the high-speed model fan. The UHB rig was powered by a high-pressure air turbine drive with the drive air and instrumentation supplied through the floor-mounted support strut, shown in figure 1. The drive turbine exhaust air was ducted downstream through an acoustically treated diffuser and exited the end of the

treated test section. There was no significant acoustic contamination of the aft fan data from the turbine exhaust.

The fan stage featured an active core, or booster stage. The booster pressure ratio was slightly lower than that for the bypass flow, and the fan bypass ratio was 5 at design speed. The fan design and flow path approximated that of the GEAE CF6 engine. The model had a simulated engine pylon and nozzle bifurcation contained within the bypass duct located circumferentially 180° apart. The simulated nozzle bifurcation strut was located in the horizontal plane on the traversing microphone side of the model. The model fan was tested with three different bypass rotors and stator sets.

Table I shows design point parameters for the high-speed fan stage. The rotor diameter was 56 cm (22 in.). Photographs of the wide chord, forward swept, and shrouded rotors are shown, respectively in figures 2 to 4. The 24 blade wide chord rotor (baseline) is representative of a GE90 engine rotor. The forward swept rotor (also 24 blades) offered the possibility of reduced MPT generation at transonic fan speeds as well as slightly increased rotor-stator spacing in the tip region. The 34 blade shrouded rotor is typical of what is currently used in the GEAE CF6 engine, where the mid-span shroud provides additional aeromechanical stability. The wide chord and forward swept rotors did not require mid-span shrouds, thus eliminating that source of rotor wake-stator interaction noise.

The baseline stator had 14° of leading edge sweep and 0° lean (table II), which is similar to what is used in the current GEAE CF6 engine design. Figure 5 shows a photograph of this stator set and a cross-sectional sketch of the fan stage with this baseline stator installed. The baseline stator had 80 vanes and therefore satisfied the cutoff criterion of reference 1. A 12-vane support strut assembly was located just downstream of the stator. Two of these strut airfoils were blended into the pylon and bifurcator strut contours.

The swept and leaned stator likewise had 80 vanes and the downstream 12-vane support strut assembly. This stator had 35° of leading edge sweep and 23° lean in the direction of fan rotation. Figure 6 shows a photograph of this stator set and a corresponding sketch of the installed stator. The rotor-stator axial spacing for the swept and leaned stator was slightly less than that for the baseline stator at the hub, and slightly greater at the tip (table II). The stator transitioned to radial (from sweep and lean) for the inner 25 percent of the span to maintain efficient aerodynamic performance.

The swept integral vane/frame stator eliminated the need for the downstream support struts (fig. 7), although the downstream support and bifurcation struts were still in place. This stator is similar to what is used in the GE90 turbofan engine. Two of these vanes were blended into the support pylon and bifurcation struts. This stator had 21° of leading edge sweep and 0° of lean. The absence of the downstream support struts enabled larger axial rotor-stator spacing than for the other two stator sets.

Anechoic Wind Tunnel and Acoustic Instrumentation

The NASA Glenn 9- by 15-Foot LSWT is located in the low speed return leg of the 8- by 6-Foot Supersonic Wind Tunnel. The tunnel test section walls, floor, and ceiling have acoustic treatment to produce an anechoic test environment (refs. 9 to 11). Figure 8 is a sketch of the test fan installed in the 9- by 15-Foot LSWT. Sideline acoustic data were acquired with a computer-controlled translating microphone probe (also seen in the photograph of fig. 1) and with three aft microphone assemblies mounted to the tunnel floor. The translating microphone probe acquired data at 48 sideline geometric angles from 27.2 to 134.6° relative to the fan rotor plane. The translating probe traverse was 227 cm (89 in.) from the fan rotational axis (about four fan diameters). A wall microphone assembly placed a reference microphone adjacent to the translating probe home position (134.6°, maximum aft travel). The three fixed microphone assemblies were mounted at the home axial position to acquire aft acoustic data at geometric angles of 140, 150, and 160°. Data were also acquired with an acoustic barrier wall installed adjacent to the fan which effectively blocked aft-radiated fan noise (fig. 9).

The acoustic data were acquired through a digital computer system and stored for post-run processing and analysis. Repeat data were acquired for two of the rotor-stator combinations during the course of this test series. In each case the repeat data were for a separate "rebuild" of the rotor-stator configuration. The repeatability of the far-field acoustic data, on an overall sound power level basis, was typically 0.5 dB.

Results and Discussion

Aerodynamic Performance

The three stator sets were designed for equivalent aerodynamic performance. Figure 10 presents the fan operating map for the three stator sets with the wide chord rotor. Acoustic data were taken on the "acoustic operating line," which was sized for maximum takeoff thrust at sea level conditions. The fan maps (stage pressure ratio vs corrected weight flow) were generated from corresponding aerodynamic runs employing a bellmouth inlet and extensive aerodynamic instrumentation. The approach, cutback and takeoff fan speeds were designated, respectively, as 61.8, 84.5, and 100 percent of fan design speed (see table III). Acoustic data were taken with a flight inlet. Limited aerodynamic instrumentation was available to verify the fan operating line. The swept and leaned stator performed slightly better than the other two stator sets (higher pressure ratio/weight flow at a particular rotor speed). References 12 to 14 present detailed aerodynamic results for this fan test. Reference 12 shows the swept and leaned stator to be nominally 2 percent higher in adiabatic efficiency on the acoustic fan operating line relative to the other two stators for most rotor test speeds, with the efficiency differences becoming smaller near 100 percent corrected fan speed. The performance for the three stator sets was basically similar from the stall region to the acoustic operating line. The performance difference does become significant in the choke region (below the design operating line), especially at intermediate fan speeds.

Figures 11 and 12 present the corresponding fan operating maps respectively for the three stator sets and the forward swept and shrouded rotor. These results show essentially the same performance variation with stator set as was seen in figure 10 for the wide chord rotor.

The original intention of these test fan stages was to have similar stage flow and pressure ratios at the same rotational speed. However, design iterations resulted in the forward swept rotor showing a somewhat higher flow and pressure ratio than did the other two rotors at corresponding fan speeds. This is clearly seen in the fan operating maps of figures 13 to 15 which compare performance for the three rotors with, respectively, the baseline radial swept, swept and leaned, and integral vane/frame stators. The aerodynamic performance of the shrouded rotor was close to that of the baseline rotor at the design operating line; however, the shrouded rotor typically showed a lower stage pressure ratio toward stall.

Acoustic Performance

All of the fan acoustic data were acquired at 0.10 tunnel Mach. Sideline data are presented in terms of emission angles. The emission angles are related to the geometric, or observed angles by the relationship:

$$\Theta_{em} = \Theta_{geom} - \sin^{-1}\left(M_0 \sin \Theta_{geom}\right)$$

where Θ_{em} and Θ_{geom} are, respectively, the emission and observed sideline angles, and M_0 is the test section Mach number. The observed angles for the sideline translating microphone probe are then

25 to 130°, and the three fixed microphones measure aft observed angles are 136, 147, and 158°. This angular range was sufficient to define the sideline noise profile for this aft-dominated fan for subsequent EPNL calculations.

Digital acoustic data were processed as constant bandwidth spectra. Time histories were acquired and averaged at each translating probe or fixed mic position with 6 and 59 Hz bandwidths. These constant bandwidth spectra were electronically merged and used to generate 1/3-octave spectra. A flyover Effective Perceived Noise Level code was used to generate relative flyover EPNL values at a 457 m (1500 ft) altitude. The code could selectively remove spectral tones to show relative EPNL changes associated with removal of bypass and core rotor/vane interaction tones. Results from this analysis code show relative EPNdB values for various configurations, and are not intended to be representative of any particular aircraft.

Sound pressure level spectra.—Figure 16 shows representative upstream (50° emission angle) and downstream (121° emission angle) constant (59 Hz) bandwidth spectra for the baseline stator at selected fan speeds. Upstream (50° emission angle) spectra are presented with and without the acoustic barrier wall in place. Downstream spectra are not relevant with the barrier wall in place. The dominant tones for spectra at 50 percent design fan speed (fig. 16(a)) are the core IGV-rotor BPF and 2BPF tones in the downstream spectra. The core IGV-rotor interaction is cut on (see table II) and the IGV-rotor spacing is quite close. Note that there is little evidence of these tones in the upstream spectra. The bypass rotor-stator interaction tones are cutoff and of little significance in these spectra.

These first two core rotor tones are likewise prominent in the downstream spectra at the designated approach, 61.8 percent fan speed (fig. 16(b)). The fundamental (BPF) bypass rotor tone is seen in the upstream spectra. The source of this tone is not clear. The blade to vane numbers (24, 80) would indicate that this tone is strongly cut off at this fan speed. However, the downstream struts would be cut on. The support and bifurcation struts would effectively appear as 2 vanes. Also, the downstream 12-vane support frame would be cut on. These types of interaction tones have been observed in previous fan tests (refs. 15 to 17). Rotor-inflow interaction noise is also a possibility.

Analytical removal of the bypass rotor tones was shown to be substantially effective at 80 percent design fan speed, which is just below designated cutback. Figure 16(c) shows representative spectra at that fan speed. Although still present, core tones are less important at this fan speed, due in part to the higher overall noise levels. Rotor multiple pure tones (MPT), typical of transonic operation, are seen in these spectra. MPT tones are generated by rotor shock waves, resulting in coherent radiated tones at multiples of the shaft rotation frequency. The bypass fundamental tone (which is strongly rotor generated at supersonic tip speeds) is prominent in these spectra.

The designated cutback fan speed was 84.5 percent of design (fig. 16(d)). The bypass fundamental tone is still prominent—especially in the upstream spectra. The core fundamental tone is evident in the downstream spectra. The bypass BPF tone is the only strong tone present at 100 percent design fan speed (fig. 16(e)) and is seen in spectra for all three stator sets at this fan speed.

Core tone contribution.—There is significant evidence that the core IGV-rotor interaction tones are predominantly aft-radiating. The active core was included both for aerodynamic considerations and to better model an actual engine application. However, aft-radiating core noise would likely be attenuated in the engine turbomachinery and therefore not be a factor in far-field noise.

The SPL spectra of figure 16 suggest that the core interaction tones are primarily present in aft radiated noise. Figure 17 shows the constant bandwidth (59 Hz) SPL directivity for the core BPF tone at 60.8 percent fan speed (no barrier wall present) for the wide chord rotor and baseline stator. The core tone is typically highest toward the downstream sideline angles. This conclusion is typical for all fan test speeds, although the core BPF directivity is only shown for 60.8 percent fan speed in figure 17.

The acoustic barrier wall has been shown to effectively block aft radiating noise from the model turbofan. Therefore, a comparison of sideline core tone noise levels with/without the barrier wall present should show the significance of forward radiating core noise. The impact of the core noise on effective

perceived noise levels (EPNL) for the wide chord rotor is shown in figure 18 (without the barrier wall present) and figure 19 (barrier wall installed). Noise levels are shown for the core BPF tone removed, and all core interaction tones (nBPF) removed relative to noise levels with all core tones present. The presence of the core tones can contribute almost 2 EPNdB at lower (subsonic) fan tip speeds. In contrast, removal of the core interaction tones had a negligible effect on EPNL calculated with the barrier wall present (based on forward radiating noise). Thus it is clear that the core stage interaction noise is highly aft radiating and may unrealistically mask acoustic benefits associated with bypass noise reduction. Consequently, EPNL results presented in this report will be with the core interaction tones analytically removed from the acoustic spectra.

Sound power level.

PWL spectra comparing three stators: Sound power level spectra (PWL) integrate the entire far-field noise data and, therefore, provide a good summary of the fan noise. The PWL integration is taken from the lossless microphone data and assumes cylindrical symmetry at the respective sideline angles. Acoustic energy upstream and downstream of the range of sideline measurement angles is ignored and assumed to be insignificant in the sound power calculations.

Figure 20 shows PWL spectra (59 Hz bandwidth, lossless data) for the wide chord rotor and three stator sets. Figure 20(a) shows spectra at 50 percent design fan speed. These spectra are dominated by the core BPF and 2BPF tones. The swept and leaned and swept integral vane/frame stators lowered broadband levels by 2 to 3 dB relative to noise levels for the baseline stator, with the swept and leaned stator being somewhat more effective at lower frequencies.

The first two core tones dominate the spectra at 61.8 percent design fan speed (designated approach, fig. 20(b)). There is some spectral evidence of the bypass fundamental BPF tone, although this tone was predicted to be cutoff at subsonic fan speeds. There are a series of "sum tones" first seen between the core BPF and 2BPF tones. These tones appear at frequencies defined as the core BPF + n(bypass BPF) where n is 1, 2, 3….. These modulation tones are quite strong at this fan speed.

Sound power level spectra at 70 percent design fan speed are shown in figure 20(c). The core rotor tones continue to dominate these spectra; however the sum tones noted at 61.8 percent fan speed are less significant at this somewhat higher speed.

There was a spectral contamination near 2000 Hz due to a continuing acoustic problem with several bolt holes in the fan drive support strut. These holes were filled and covered before each run, but due to oil, etc., this covering tended to tear away during the fan run. The noise hump centered at 2000 Hz was correlated with the degeneration of these hole covers, and was a problem for the baseline and swept and leaned stator data, which were taken earlier in the test series. New hole filling procedures eventually corrected this problem. The compromised data were at 65, 70, and 75 percent of design speed due both to sensitivity to flow impingement at these fan speeds, and that these points were typically taken later in the test day when the degeneration of the hole covering was more pronounced. Directivity results at these fan speeds and frequency showed that flow noise from the exposed bolt holes was not very directional, tending to raise the SPL by 5 or more dB throughout the angular survey.

As previously mentioned, the bypass tones become strongly rotor generated at supersonic fan speeds. Figure 20(d) shows PWL spectra at 80 percent fan design speed. Both bypass and core rotor tones are evident in the PWL spectra at this fan speed. Broadband levels were still reduced with the advanced stator sets, although not as much as for subsonic fan speeds. The PWL spectra at 84.5 percent fan speed (designated cutback, fig. 20(e)) are essentially similar to those for 80 percent speed.

At 100 percent design fan speed (fig. 20(f)) the spectra are dominated by bypass rotor tones; multiple pure tones are not present. Core rotor tones are relatively insignificant at this fan speed. Broadband levels were about 1 dB lower with the swept and leaned and integral vane/frame stator sets compared to the baseline stator.

Corresponding PWL spectra for the forward swept and shrouded rotors with the three test stators are shown in figures 21 and 22. While the results are basically similar to those of figure 20 (noise reductions

associated with the swept and leaned and integral vane/frame stators), there are some differences. Additional rotor wake would be expected from the mid-span shroud of the shrouded rotor. Also, it is possible that the forward swept rotor generated more downstream wake than did the baseline, wide chord rotor (adverse flow separation, etc.).

The bypass BPF tone was present at 50 percent design fan speed for the forward swept and shrouded rotors (figs. 21(a) and 22(a)), whereas this tone and its harmonics were not present for the wide chord rotor at this fan speed. The highest bypass tone levels were with the baseline stator. The most BPF tone reduction was with the integral vane/frame stator for the forward swept rotor, and with the swept and leaned stator for the shrouded rotor.

Bypass BPF tone levels were quite strong and essentially independent of stator configuration for the forward swept rotor (fig. 21) at intermediate fan speeds (61.8 to 80 percent design), although at higher fan speeds (84.5 and 100 percent) both the swept and leaned and integral vane stators gave similar tone reductions relative to noise levels for the baseline stator.

The bypass BPF tone for the shrouded rotor (fig. 22) is significantly higher for the integral vane/frame stator than for the other two stators at fan speeds from 61.8 and 70 percent design fan speed. At higher fan speeds there is some tone reduction associated with this rotor and the swept and leaned stator. Another interesting observation is that multiple pure tone (MPT) content is highest for the shrouded rotor at transonic fan speeds (80 and 84.5 percent design). This may be due to additional shock waves being generated by the rotor mid-span shrouds.

PWL spectra comparing three rotors: Sound power level spectra comparing noise for the three rotors with each test stator are presented in figures 23 to 25. Although all three rotors had the same design rpm, the higher blade number for the shrouded rotor (34 vs 24, table II) gave a higher interaction tone frequency for that rotor at a particular fan speed.

The aerodynamic performance of the forward swept rotor was somewhat different from that of the wide chord and shrouded rotors (see figs. 13 to 15). Although designed for similar aerodynamic performance, the forward swept rotor typically showed a higher mass flow and pressure ratio at a given fan speed. This gave the forward swept rotor 2 to 3 percent higher mass flow and stage pressure ratio relative to the other two rotors at a typical fan speed, although the difference was less at design fan speed. If the noise difference follows as 10 log (PR_1/PR_2), the expected noise difference between the two rotors at a particular fan speed would be a negligible 0.1 dB. This expression for noise scaling with thrust (approximated by pressure ratio) is valid for scaling a particular fan stage, but may not be valid for scaling two different fan stages. Differences in the downstream wakes of the test rotors (not measured) could have a significant impact on rotor-downstream vane/strut noise generation.

The wide chord rotor is quietest with the baseline stator at subsonic fan tip speeds (fig. 23). Broadband levels associated with the swept and leaned and shrouded rotors are essentially identical at subsonic fan tip speeds. However, bypass tone levels tend to be higher for the forward swept rotor at subsonic fan tip speeds. This again suggests that the downstream wake for the forward swept rotor is particularly strong.

As previously seen in figure 22, MPT generation for the shrouded rotor in the transonic speed range (80 and 84.5 percent design speed) is significantly higher than that for the other two rotors. The shrouded rotor has a slightly lower broadband level at design fan speed (fig. 23(f)), but rotor-alone tone levels are similar to those for the other two rotors.

PWL spectra for the swept and leaned stator (fig. 24) essentially follow what was seen for the baseline stator in figure 23.

PWL spectra for the integral vane/frame stator shows the same relative broadband levels as were seen for the other two stators. However, the fundamental bypass tone level (BPF) at subsonic fan tip speeds is significantly higher for the shrouded rotor (rather than for the forward swept rotor as was the case for the other two stators). The mid-span shroud would certainly generate a significant wake which would not be present for the other two rotors. Also, the vane count is lower for the integral vane/frame

stator (52 vs 80) which would favor propagation of the BPF tone for this rotor-stator combination. The bypass 2BPF tone levels are more nearly the same for the three rotors at these subsonic fan tip speeds.

Figure 25 presents the corresponding PWL spectra for the integral vane/frame stator and three rotors. The bypass BPF tone levels are nearly the same for the three rotors in the transonic (80 and 84.5 percent design speed) range (fig. 25(d) and (e)). However, the bypass BPF tone level for the shrouded rotor is significantly higher than that for the other two rotors at design fan speed (fig. 25(e)). The bypass BPF tone level at design fan speed for the shrouded rotor is higher than was seen for that rotor and the other two stators (figs. 23(e) and 24(e)). The corresponding BPF tones for the other two rotors and the integral vane/frame stator at design fan speed (fig. 25(e)) were actually lower than the corresponding tones with the baseline and swept and leaned stators at design speed. Thus it is clear that the bypass BPF tone at supersonic tip speeds is influenced by rotor-downstream stator/strut interaction as well as rotor-alone generation, and that there is a significant difference in how the shrouded rotor and the other two rotors interact with the integral vane/frame stator.

Forward/aft sound power radiation: The 59 Hz bandwidth sound power level results were used to give an indication of the forward/aft noise radiation. PWL results with the acoustic barrier wall in place were considered to be exclusively from inlet radiation. An indication of the aft-radiated noise was taken as a decibel difference of the PWL with the barrier wall in place from the PWL without the barrier wall. The overall sound power level (OAPWL) was integrated from 1 to 40 kHz over the available lossless sideline data. The bypass BPF and 2BPF tone power levels were taken from inspection of the PWL spectra. It was often necessary to perform a logarithmic addition of adjacent PWL frequency bands which clearly contained the tone of interest. This technique is thought to give a reasonable result for the forward/aft sound power radiation. However, some level of error may be introduced because of subjective addition of adjacent frequency bands thought to represent the BPF and 2BPF tones. An additional error could be introduced due to the different included angular range of the far-field microphones without the barrier wall in place (25 to 158° emission angle) and with the barrier wall in place (no fixed mics, 25 to 130° emission angle). Acoustic data were not taken for the integral vane/frame stator with the barrier wall in place; hence, forward/aft sound power results were not possible for that stator.

Figures 26 to 40 present total, forward-radiating, and aft-radiating sound power as a function of rotor tangential tip speed. Plots are shown for the OAPWL as well as for the first two orders of the bypass rotor-stator interaction tone. Aft-radiated noise is typically dominant at all fan speeds, especially above transonic rotor tip speed. Inlet-radiated noise is highest and sometimes dominant in the region of transonic rotor tip speed. Results are presented analogous to the previous PWL spectra plots, showing the effect of stator configuration for a particular rotor, followed by rotor configuration for a particular stator. The integral vane/frame stator was not tested with the acoustic barrier wall in place.

The OAPWL forward/aft radiation results are shown in figures 26 to 30. In each case, the forward-radiating noise is significantly less than the aft-radiating noise except in the transonic rotor tip speed region (around 1200 ft/s), where the inlet-radiating noise approaches, but does not exceed the aft-radiating noise. The inlet-radiating noise tends to somewhat reduce in level at rotor tip speeds above transonic. The total and calculated aft-radiating noise is essentially the same throughout the fan speed range in each comparison.

Figures 31 to 35 show the forward/aft PWL split for the fundamental bypass BPF tone. The forward/aft sound power split for the wide chord rotor is shown in figure 31. Results for the baseline and swept and leaned stator show the forward and aft radiation levels to be comparable at subsonic rotor tip speeds. The aft-radiated noise tends to dominate at transonic and higher rotor tip speeds. This results contrasts with that for the forward swept and shrouded rotors (figs. 32 and 33) in which aft-radiated noise clearly dominates at sub and supersonic rotor tip speeds, although there tends to be a small region of forward-radiated noise dominance near transonic rotor tip speed.

Figures 34 and 35 show the forward/aft BPF tone PWL split for the three rotors with, respectively, the baseline and swept and leaned stators. The forward and aft-radiating noise levels tend to be about the same for the wide chord rotor at subsonic tip speeds, with the aft-radiating noise dominating in all cases at supersonic rotor tip speeds.

Figures 36 to 40 show the forward/aft PWL split for the first harmonic bypass 2BPF tone. The 2BPF tone levels tend to be aft-dominating for the wide chord rotor and baseline stator at all fan speeds (fig. 36) except in the transonic region where the forward/aft split is about the same. The aft-radiating 2BPF tone is highly aft-dominant for the forward swept and shrouded rotors (figs. 37 and 38). Figures 39 and 40 show the 2BPF PWL split for the baseline and swept and leaned stators, respectively with the three stator sets. The forward swept and shrouded rotor show the strongest aft dominance for the 2BPF tone.

Effective perceived noise level.—An effective perceived noise level (EPNL) script was used which "flew" the model fan at a 1500 ft altitude and 0.10M. The acoustic data used a 3.35 scaling factor to adjust the data to a representative full-scale engine size. The EPNL results are intended to give relative noise values and are not representative of a particular aircraft or flight profile. The core stage interaction tones were previously shown to be almost exclusively aft-radiating and therefore would be absorbed by downstream turbomachinery within an actual turbofan engine. These core tones have been analytically removed for all of the following EPNL results. EPNL were calculated with all of the bypass interaction tones present, the fundamental bypass rotor interaction tone (BPF) electronically removed, and with all harmonics of that tone (nBPF) electronically removed. EPNL values are presented as a function of rotor tip speed both as calculated levels, and as a difference from the reference wide chord rotor and baseline stator with all bypass tones present.

Comparison to the baseline configuration—wide chord rotor: Figure 41 shows EPNL for the wide chord rotor and baseline stator. The bypass interaction tones (BPF and nBPF) tend to be significant only in the transonic blade tip speed region (nominally 1100 to 1300 ft/sec), where removal of these tones results in a 4 to 5 EPNdB noise reduction. Removal of these bypass tones is of little significance at subsonic and supersonic rotor tip speeds.

As shown in figure 42, the swept and leaned stator with the wide chord rotor gave a 2.5 EPNdB noise reduction relative to the baseline stator at subsonic tip speeds below 950 ft/sec, and a modest 1 to 1.5 EPNdB reduction at supersonic tip speeds. Removal of the bypass interaction tones in the transonic tip speed region again gave a 4 to 5 EPNdB reduction relative to the reference baseline configuration.

The integral vane/frame stator with the wide chord rotor (fig. 43) gave noise reductions of about 2 EPNdB at subsonic rotor tip speeds, which was almost as much as was seen for the swept and leaned stator at these tip speeds. Removal of the bypass interaction tones in the transonic tip speed region was slightly more effective than for the other two stators, giving 5 and 6 EPNdB reductions, respectively, for removal of the BPF and nBPF tones.

Comparison to the baseline configuration—forward swept rotor: Similar EPNL comparisons for the forward swept rotor and three stator sets are shown in figures 44 to 46. The forward swept rotor typically had higher noise levels than did the wide chord rotor as was seen in the previous PWL spectra. Perceived noise levels for the forward swept rotor and baseline stator (fig. 44) are about 2 EPNdB higher than for the wide chord rotor and baseline stator at rotor tip speeds below transonic. Although present in the PWL spectra, removal of the bypass interaction tones had little effect on the subsonic tip speed EPNL, suggesting that broadband noise is a major factor for the forward swept rotor. Removal of bypass interaction tones in the transonic tip speed region did significantly reduce the EPNL, but this configuration still remains noisier than the wide chord rotor configurations with similar tone removal.

The acoustic performance of the forward swept rotor was significantly better with the swept and leaned stator (fig. 45). The noise levels with this configuration were essentially the same as for the reference baseline configuration (wide chord rotor and baseline stator) at subsonic tip speeds below 950 ft/sec. Bypass tone removal gave little improvement at subsonic tip speeds. The presence of the

swept and leaned stator reduced broadband noise levels by about 2 EPNdB. Removal of the bypass interaction tones in the transonic tip speed region gave a 4 to 5 EPNdB reduction, which again was similar to reductions shown for the baseline configuration with tone removal.

Noise levels for the forward swept rotor and integral vane/frame stator (fig. 46) were slightly higher than for the reference baseline configuration at subsonic tip speeds, and removal of the bypass interaction tones was again effective in the transonic tip speed region.

Comparison to the baseline configuration—shrouded rotor: The shrouded rotor was the noisiest rotor with the baseline stator at subsonic rotor tip speeds (fig. 47), being up to 4 EPNdB noisier than the baseline configuration at rotor speeds below approach. Bypass tone removal helped somewhat, but only to bring the subsonic tip speed EPNL to values comparable to those seen for the forward swept rotor and baseline stator. Curiously, noise levels for the shrouded rotor and baseline stator were slightly below reference baseline levels in the transonic tip speed region. Bypass tone removal was somewhat reduced noise levels in the transonic through supersonic tip speed region, although noise levels were still higher than for the baseline configuration with similar tone removal in the transonic region. Tone removal at supersonic rotor tip speeds (BPF tone removal was sufficient) was more beneficial for this rotor-stator combination than it was for the other two rotors, suggesting that broadband levels associated with the shrouded rotor at supersonic tip speed are somewhat lower than those for the other two rotors.

The swept and leaned stator was effective in reducing noise levels for the shrouded rotor to reference baseline levels at subsonic rotor tip speeds (fig. 48). Again, the noise reduction associated with the swept and leaned stator appears to be due to reductions in broadband rather than interaction tone noise. The acoustic behavior of the shrouded rotor in the transonic tip speed region with the swept and leaned stator was significantly different than was seen for the other two rotors (see figs. 42 and 45). In particular, noise levels for the other two rotors and the swept and leaned stator in the transonic rotor tip speed region were essentially the same as for the baseline configuration. However, the swept and leaned stator gave almost a 4 EPNdB reduction with the shrouded rotor near 1200 ft/sec rotor tip speed without electronic tone removal. Removal of the bypass BPF tone gave an additional 1 EPNdB.

Noise levels for the shrouded rotor and integral vane frame stator (fig. 49) were as much as 3 EPNdB higher than baseline levels except at the transonic rotor tip speed region where the noise dipped to baseline levels. Removal of the bypass BPF tone was effective throughout the range of rotor tip speeds; however removal of additional tones was of no additional benefit except at the lowest rotor tip speeds.

Comparison of three rotors—baseline stator: Figures 50 to 52 show relative EPNL for the three test rotors and the baseline stator. Again, the acoustic reference is the wide chord rotor and baseline stator with all bypass tones present. EPNL results are shown, respectively, with all bypass tones present, the fundamental BPF tone electronically removed, and all nBPF tones removed.

Figure 50 shows that noise levels for the forward swept and shrouded rotor are significantly higher than those for the baseline rotor when all bypass tones are present. In particular, subsonic noise levels are 2 to 2.5 EPNdB higher than reference levels for these stators at subsonic rotor tip speeds. Noise levels for the forward swept rotor, in particular, remain quite high relative to baseline levels through rotor tip speeds somewhat above transonic.

Removal of the fundamental bypass interaction tone, BPF, was helpful in the transonic tip speed region (fig. 51) being marginally effective for the forward swept rotor and most effective for the wide chord rotor. BPF tone removal was helpful for the shrouded rotor at supersonic tip speeds.

Removal of all bypass interaction tones, nBPF, was particularly helpful for the forward swept rotor (fig. 52) at transonic and higher rotor tip speeds.

Comparison of three rotors—swept and leaned stator: Figures 53 to 55 show relative EPNL for the three test rotors and the swept and leaned stator. The swept and leaned stator only showed a noise reduction at subsonic rotor tip speeds with the wide chord rotor (fig. 53). Noise reductions for the wide chord rotor at subsonic rotor tip speeds must be primarily broadband in nature since tone content was relatively insignificant at these lower speeds.

At transonic rotor tip speeds only the shrouded rotor showed a significant noise reduction with the swept and leaned stator relative to reference baseline levels. Here it would appear that the swept and leaned stator is particularly effective in reducing tone content as generated by this rotor.

Removing the bypass BPF tone (fig. 54) was effective for the wide chord and forward swept rotors in the transonic tip speed region, bringing those levels down to those for the shrouded rotor (without tone removal). There was minimal additional benefit in removing all bypass tones (nBPF, fig. 55).

Comparison of three rotors—integral vane/frame stator: Finally, figures 56 to 58 show relative EPNL for the three test rotors and the integral vane/frame stator. The noise levels for the integral vane stator varied significantly with the test rotor. Noise levels with all bypass tones present were lowest with the wide chord rotor at subsonic fan tip speeds (fig. 56), being 2 to 3 EPNdB below the reference noise level. Noise levels were clearly highest for the shrouded rotor at subsonic tip speeds. (Unlike corresponding results for the other two stators for which the forward swept and shrouded rotors showed similar high noise levels compared to the wide chord rotor.

Noise levels at 1180 ft/sec (transonic condition) were nearly the same for all three rotors. However, at higher, supersonic tip speeds, the forward swept rotor was up to 2.5 EPNdB above the reference baseline level, while the other two rotors were typically at or below the baseline level.

Removal of the fundamental bypass tone (BPF) was quite effective near the transonic tip speed condition for all three test rotors (fig. 57), lowering the EPNL by 4 to 5 EPNdB. Removal of this tone lowered the noise for the shrouded rotor at supersonic rotor tip speeds from 2.5 EPNdB above baseline reference to 2 EPNdB below the noise reference. Removal of all bypass tones (nBPF, fig. 58) was only effective in slightly reducing noise levels at transonic rotor tip speeds.

Conclusions

The acoustic characteristics of a model high-speed fan stage were measured in the NASA Glenn 9- by 15-Foot LSWT at takeoff-approach flight conditions. Acoustic results were acquired for three test rotors in combination with three stator sets. Any combination of rotor and stator could be tested. All three test rotors were designed for a rotor tip speed of 1450 ft/sec and similar weight flow. These test rotors included a “wide chord,” a forward swept rotor, and a shrouded (mid-span damper) rotor. The model fan had a core flow simulation, or booster stage, giving the model a bypass ratio of 5.

The fan was tested with three stator sets to evaluate acoustic benefits associated with a swept and leaned stator and with a swept integral vane/frame stator which incorporated some of the swept and leaned features as well as eliminated some of the downstream support structure. The baseline stator had modest aft sweep (14). The fan with the shrouded rotor and baseline stator approximated current GEAE CF6 engine design. The wide chord rotor and integral vane/frame stator was representative of GE90 engine design. The model also had a simulated support pylon and bifurcation strut in the bypass flow path.

Analysis of the far-field acoustic results showed that rotor-vane interaction tones from the core stage were strongly aft radiating. Aft-radiated core noise should be absorbed in the downstream turbomachinery of an actual engine installation. Therefore, all core rotor tones were analytically removed from the acoustic data to facilitate a more accurate appraisal of acoustic benefits associated with the modified bypass stator sets.

A flyover effective perceived noise level code was used to calculate relative EPNL values for the various configurations. Flyover EPNL results for the wide chord rotor with the swept and leaned stator relative to the baseline stator showed a 3 EPNdB reduction at subsonic fan speeds. Reductions of about 1 EPNdB were typical at transonic and higher fan speeds. The integral vane frame stator showed a 2 EPNdB reduction at these lower fan speeds and about 1.5 EPNdB at supersonic fan tip speeds.

Removal of the rotor-stator fundamental BPF tone was shown to offer a significant EPNL reduction near the cutback fan speed, with the maximum benefit associated with this tone removal at a fan speed slightly below designated cutback. Removal of this tone showed a 4 EPNdB reduction for the baseline and the swept and leaned stator, and a 6 EPNdB reduction for the swept integral vane/frame stator. (An additional noise reduction of only 1 EPNdB was achieved by removing all higher rotor-stator tone harmonics for the baseline and swept and leaned stator; removing all harmonics of the rotor tones had no further benefit for the swept integral vane/frame stator.) This result clearly shows that BPF tone elimination techniques such as active noise control or a tuned liner could offer a significant noise reduction near the cutback fan speed.

References

1. Tyler, J.M., and Sofrin, T.G., "Axial Flow Compressor Noise Studies," SAE Trans., vol. 70, 1962, pp. 309–332.
2. Woodward, R.P., and Glaser, F.W., "Wind Tunnel Measurements of Blade/Vane Ratio and Spacing Effects on Fan Noise," AIAA Journal of Aircraft, vol. 20, no. 1, January 1983, pp. 58–65.
3. Kazin, S.B., "Radially Leaned Outlet Guide Vanes for Fan Source Noise Reduction," NASA CR-134486, November 1973.
4. Envia, E., Huff, D.L., and Morrison, C.R., "Analytical Assessment of Stator Sweep and Lean in Reducing Rotor-Stator Tone Noise," AIAA–96–1791, May 1996.
5. Woodward, R.P., Elliott, D.M., Hughes, C.E., and Berton, J.J., "Benefits of Swept and Leaned Stators for Fan Noise Reduction," AIAA–99–0479.
6. Woodward, R.P., Gazzaniga, J.A., Bartos, L.J., and Hughes, C.J., "Acoustic Benefits of Stator Sweep and Lean for a High Tip Speed Fan," AIAA–2002–1034.
7. Chestnut, D., "Flight Effects of Fan Noise," NASA CP-2242, January 1982.
8. Balan, C., and Hoff, G.E., "Propulsion Simulator for High Bypass Turbofan Performance Evaluation," SAE Paper 931410, January 1993.
9. Dahl, M.D., and Woodward, R.P., "Comparison Between Design and Installed Acoustic Characteristics of the NASA Lewis 9- by 15-Foot Low Speed Wind Tunnel Acoustic Treatment," NASA TP-2996, April 1990.
10. Dahl, M.D., and Woodward, R.P., "Background Noise Levels Measured in the NASA Lewis 9- by 15-Foot Low Speed Wind Tunnel," NASA TP-3274, November 1992.
11. Woodward, R.P., and Dittmar, J.H., "Background Noise Levels Measured in the NASA Lewis 9- by 15-Foot Low-Speed Wind Tunnel," NASA TM-106817, AIAA–95–0720, January 1995.
12. Gazzaniga, J.A., "Performance of Advanced Fan Exit Guide Vane Concepts for High Speed Fans," AIAA–2002–0377.
13. Gazzaniga, J.A., "Performance of Advanced Fan Exit Guide Vanes with a Product Derived Fan," AIAA–2003–1067.
14. Gazzaniga, J.A., "Performance of Advanced Fan Exit Guide Vanes with a Product Derived Fan," AIAA–2004–0685.
15. Woodward, R.P., and Balombin, J.R., "Tone Generation by Rotor-Downstream Strut Interaction," AIAA Journal of Aircraft, vol. 21, no. 2, February 1984, pp. 135–142.
16. Sutliff, D.L., Konno, K.E., and Heidelberg, L.J., "Duct Mode Measurements on the TFE731-60 Full Scale Engine," NASA/TM—2002-211573.
17. Heidelberg, L.J., "Comparison of Tone Mode Measurements for a Forward Swept and Baseline Rotor Fan," AIAA–2003–3293.

TABLE I.—AERODYNAMIC DESIGN POINT

Fan Tip Diameter, cm (in.)	56 (22)
Corrected Tip Speed m/s (ft/s)	442 (1450)
Corrected RPM (100 percent)	15,105
Corrected Fan Airflow Kg/s (lbm/s)	45.4 (100)
Fan Inlet Radius Ratio	0.310
Specific Flow, kg/s-m^2 (lbm/s-ft^2)	1.77 (41.9)
Blade Tip Relative Mach No.	1.48
Fan Pressure Ratio (Core/Bypass)	1.64/1.76
Bypass Ratio	5.00
Booster Flow Kg/s (lbm/s) (Corrected to P_{tot} upstream of rotor)	7.56 (16.67)
Booster Overall Pressure Ratio	1.740

TABLE II.—BLADE/VANE PARAMETERS

Rotor

Design	Number of Blades	Leading Edge Sweep	Design Tip Speed, ft/s	Design Stage Pressure Ratio	Solidity at Pitch
Wide Chord	24	0° (Radial)	1450	1.76	1.87
Forward Swept	24	25°	1450	1.76	2.10
Shrouded*	34	0° (Radial)	1450	1.76	1.69

* GEAE IR&D

Stator

Design	Number of Vanes	Leading Edge Sweep	Lean	Solidity at Pitch	12 Strut Frame	Axial Spacing, (Rotor chords)	
						Hub	Tip
Radial Swept, Baseline	80	14°	0°	1.87	YES	0.76	2.54
Swept and Leaned	80	35°	23°	2.10	YES	0.62	2.72
Integral Vane/Frame	52	21°	0°	2.10	NO	1.21	3.38

Core Booster
(Fan stage includes active core (booster) flow path)

Blade/Vane	# Blades/Vanes
Inlet Guide Vanes	98
Booster Rotor	62
Deswirl Vanes	132

TABLE III.—COMMUNITY NOISE RATING CONDITIONS

Condition	Corrected Tip Speed (ft/s)	Corrected RPM	Corrected Speed, Percent Design	Corrected Mass Flow* (lbs/s)	Stage Pressure Ratio
Design Point	1450	15,105	100	100.0	1.760
Sideline	1405.7	14,637	96.9	96.3	1.732
Cutback	1224.7	12,764	84.5	81.2	1.502
Approach	896.4	9,335	61.8	55.5	1.235

* Along a sea level operating line

Figure 1.—Photograph of research fan installed in the NASA Glenn 9- by 15-Foot Low Speed Wind Tunnel.

Figure 2.—Photograph of the wide chord rotor (pressure side left; suction side right).

Figure 3.—Photograph of the forward swept rotor (pressure side left; suction side right).

Figure 4.—Photograph of the shrouded rotor (pressure side left; suction side right).

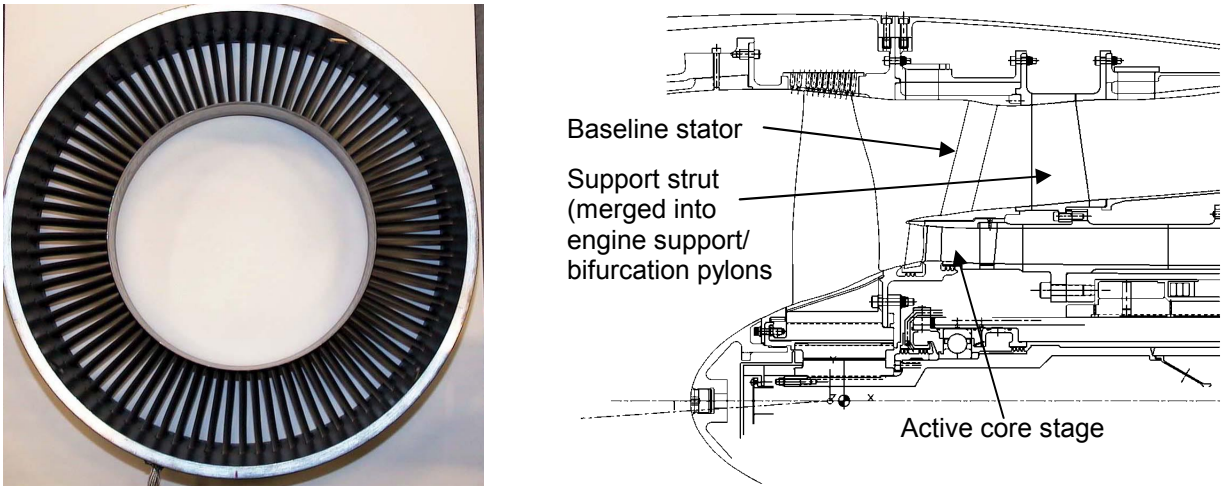

Figure 5.—Photograph of the baseline vanes (viewing downstream) along with a sketch of the fan stage with the wide chord rotor and this stator.

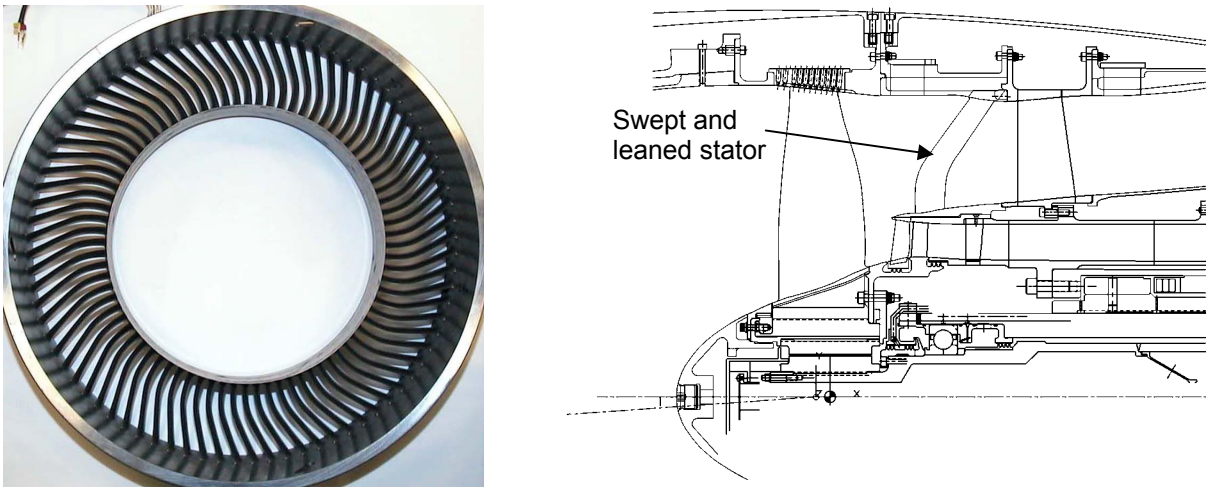

Figure 6.—Photograph of the swept and leaned vanes (viewing downstream) along with a sketch of the fan stage with the wide chord rotor and this stator.

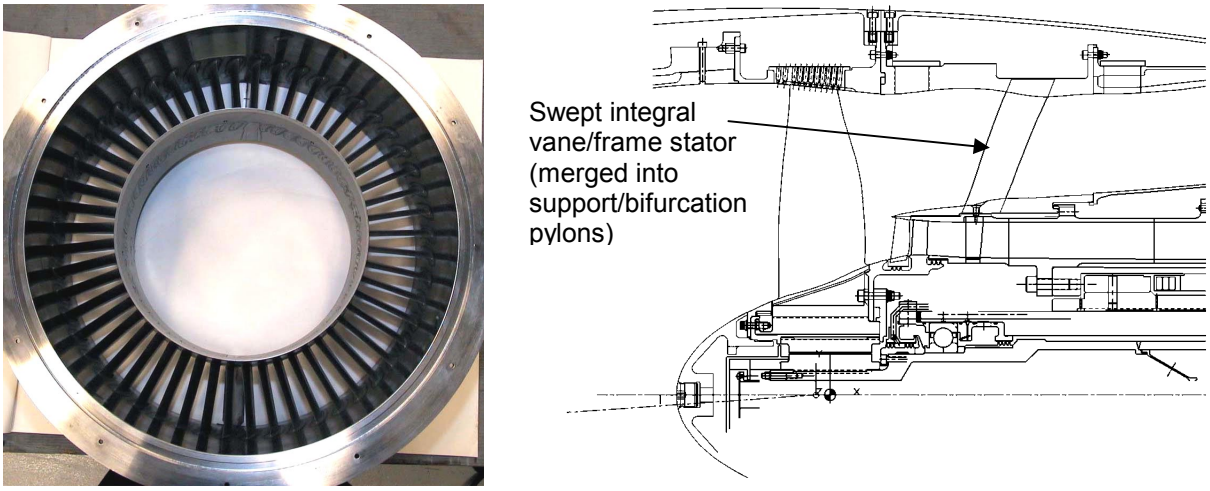

Figure 7.—Photograph of the swept integral vane/frame stator (viewing downstream) along with a sketch of the fan stage with the wide chord rotor and this stator.

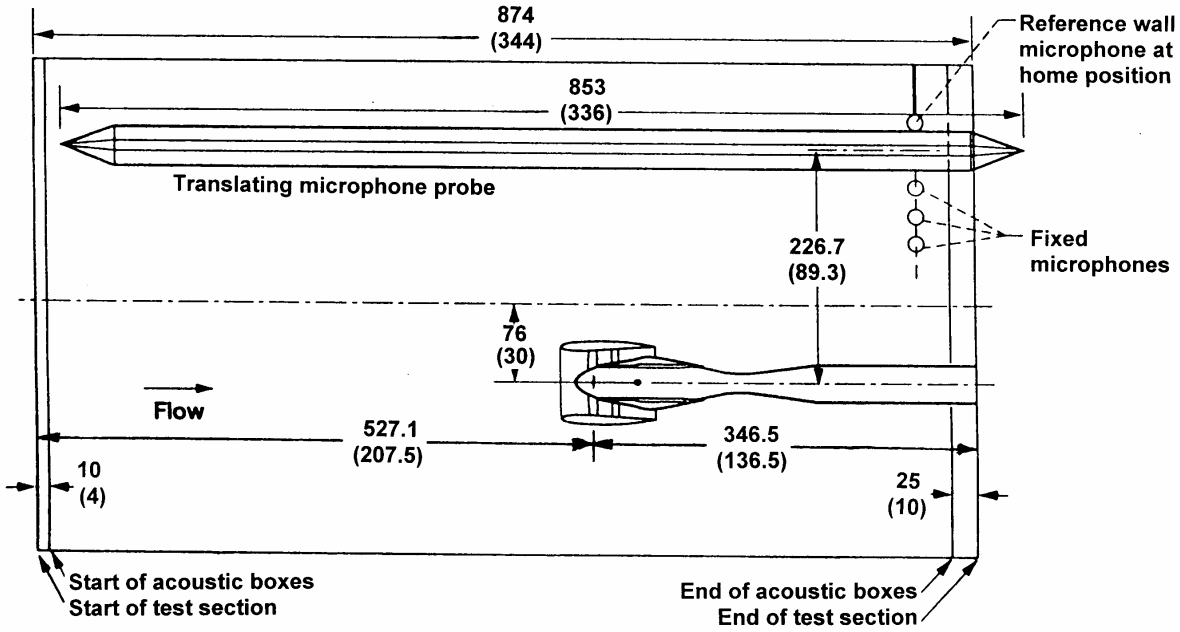

Figure 8.—Sketch of the model fan installed in the 9- by 15-Foot Low Speed Wind Tunnel. Far-field acoustic data were acquired with a translating microphone probe and aft fixed microphones. (Dimensions in cm (in.)).

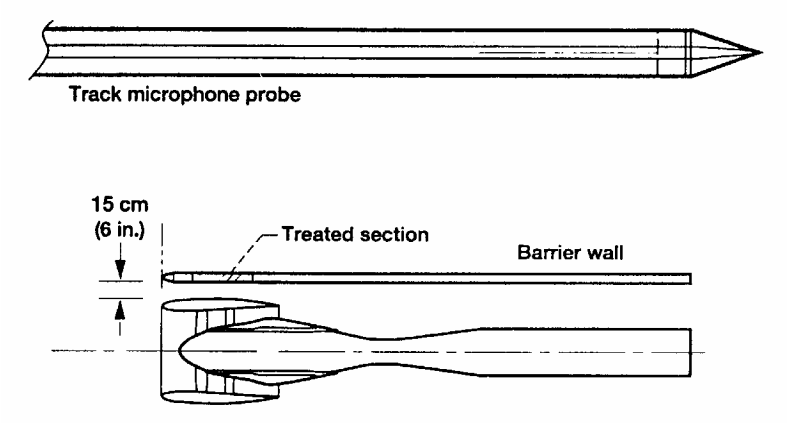

Figure 9.—Sketch showing location of acoustic barrier wall relative to model fan. (Dimensions in cm (in.)).

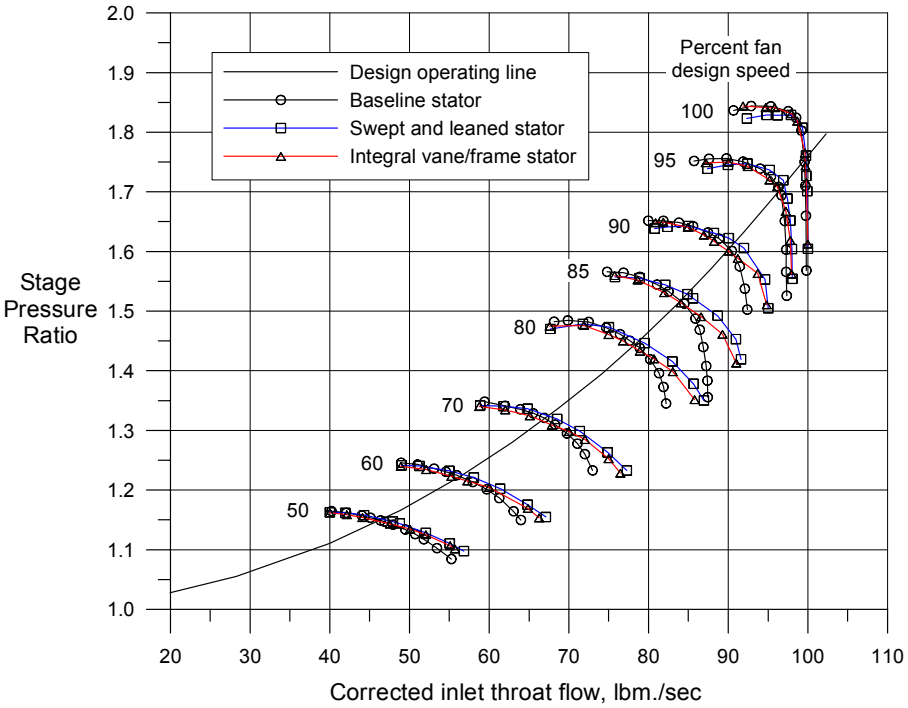

Figure 10.—Fan operating map for the wide chord rotor and three research stator sets.

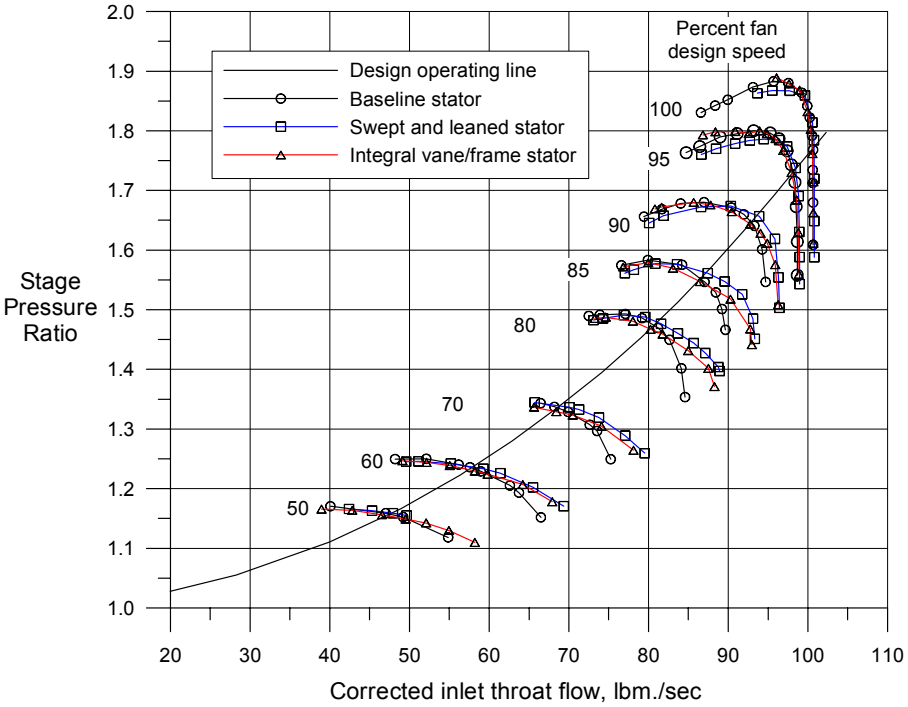

Figure 11.—Fan operating map for the forward swept rotor and three research stator sets.

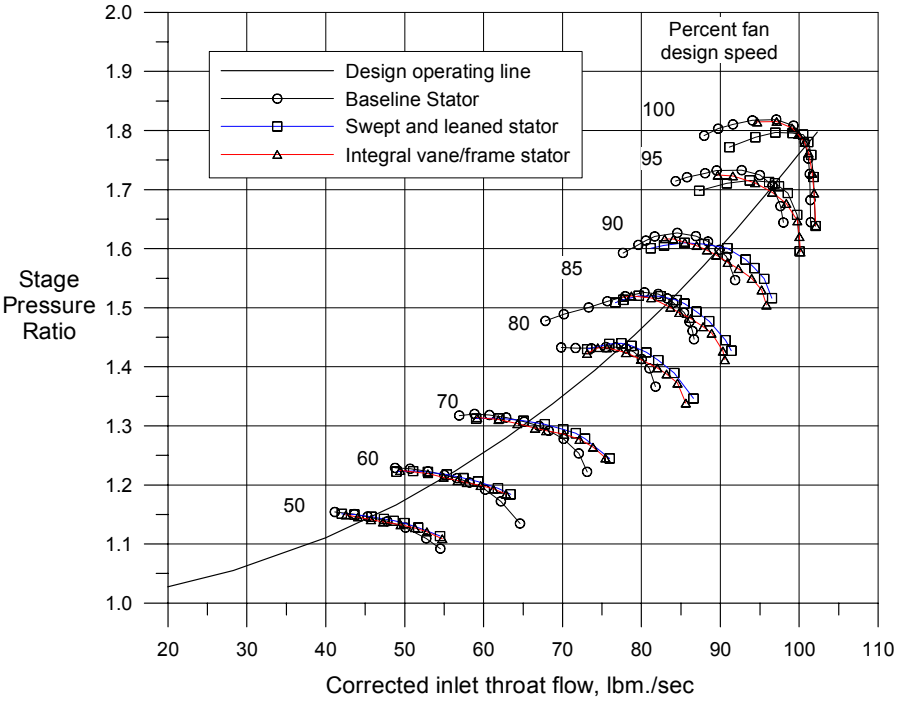

Figure 12.—Fan operating map for the shrouded rotor and three research stator sets.

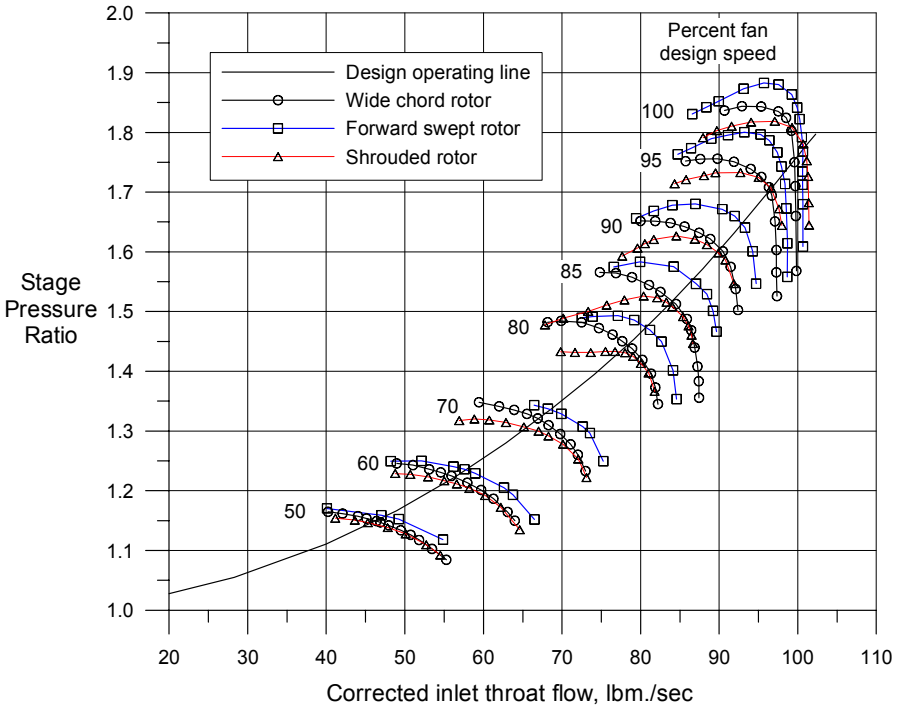

Figure 13.—Fan operating map for the baseline radial swept stator and three rotors.

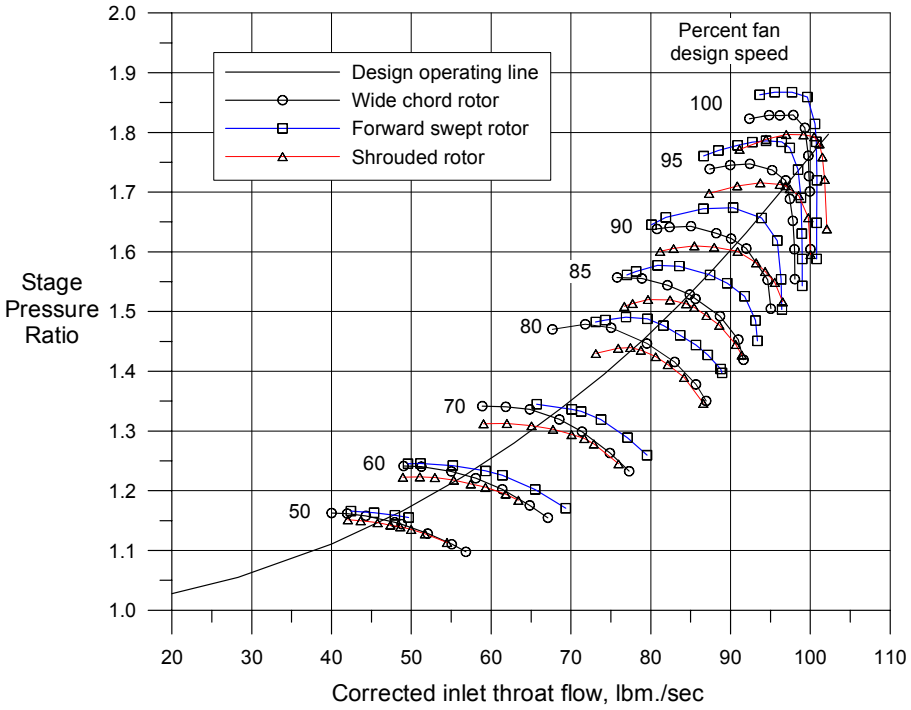

Figure 14.—Fan operating map for the swept and leaned stator and three rotors.

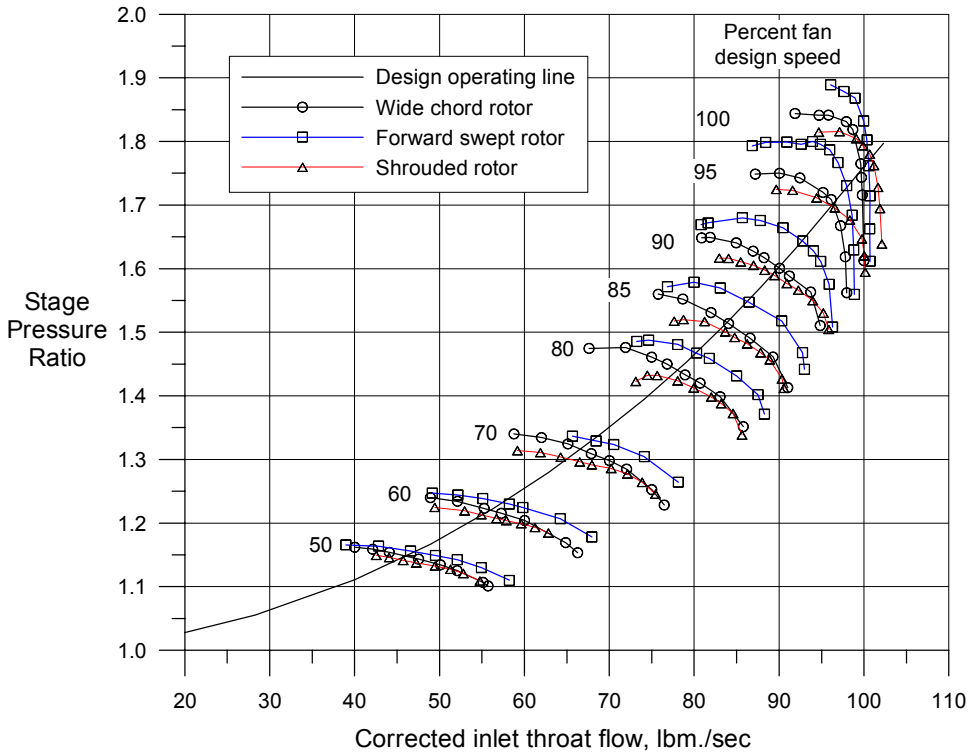

Figure 15.—Fan operating map for the integral vane/frame stator and three rotors.

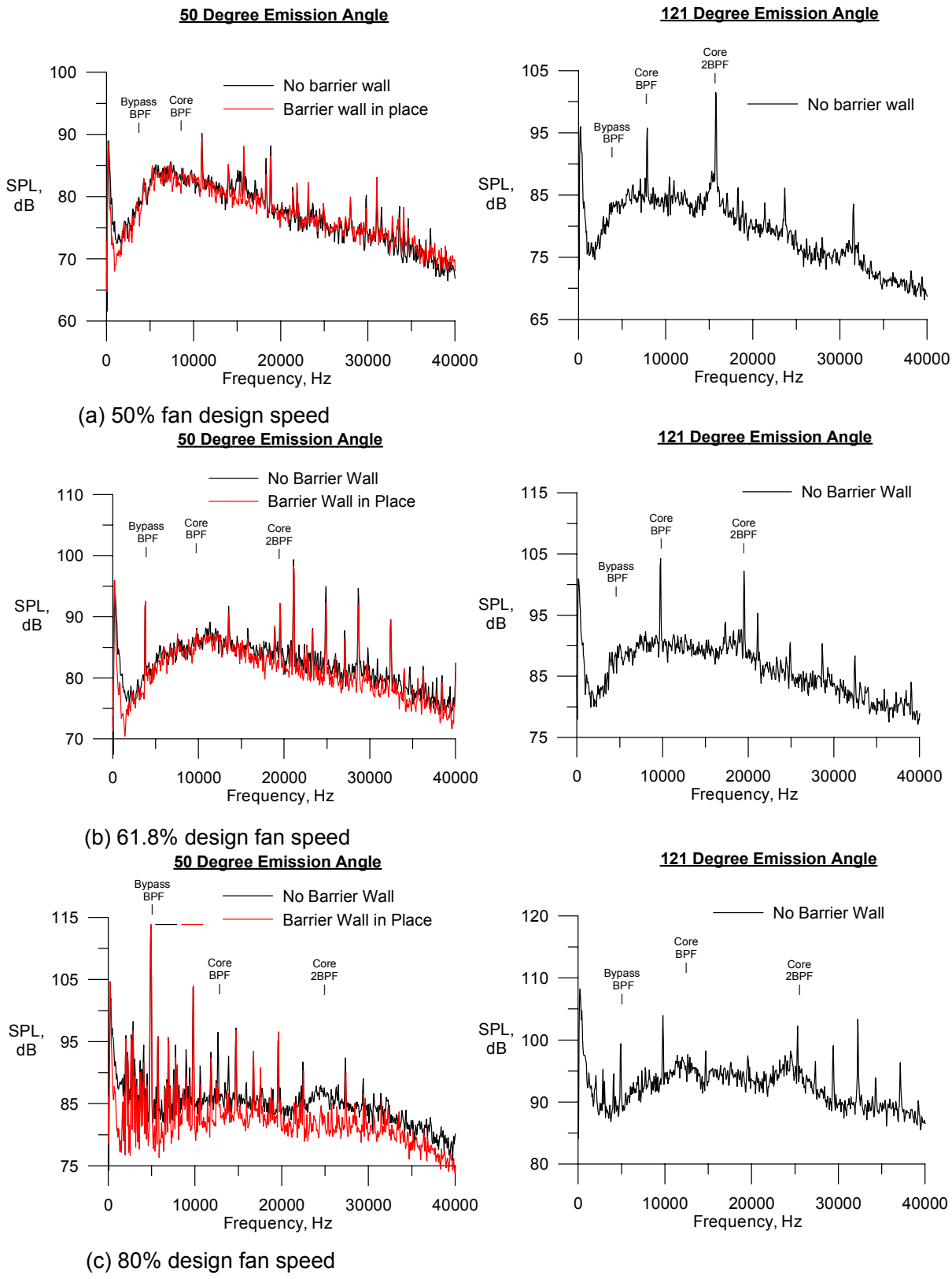

Figure 16.—Constant (59 Hz) bandwidth sound pressure level spectra.
(wide chord rotor, baseline stator, lossless data on an 89-in. sideline).

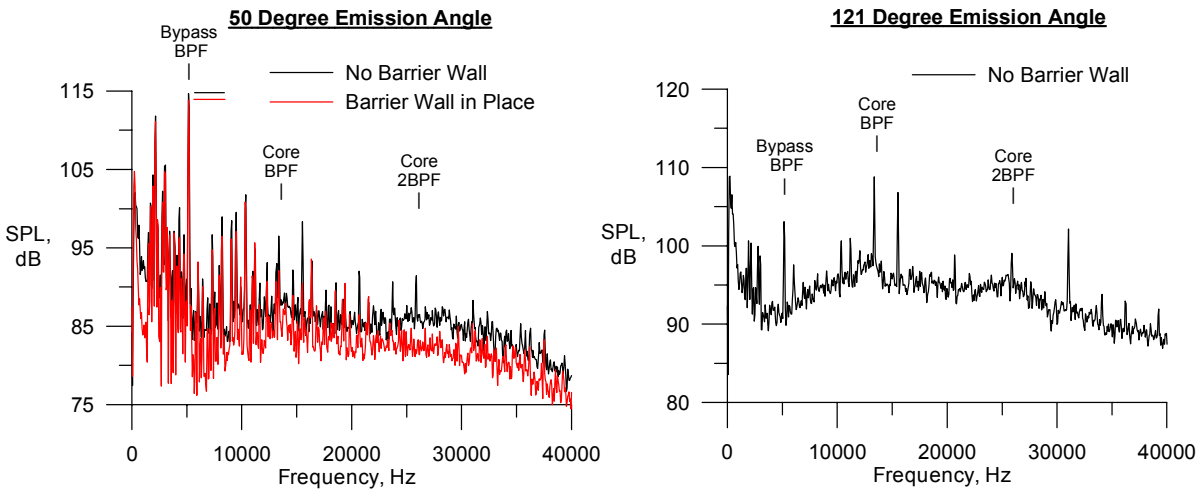

(d) 84.5% design fan speed

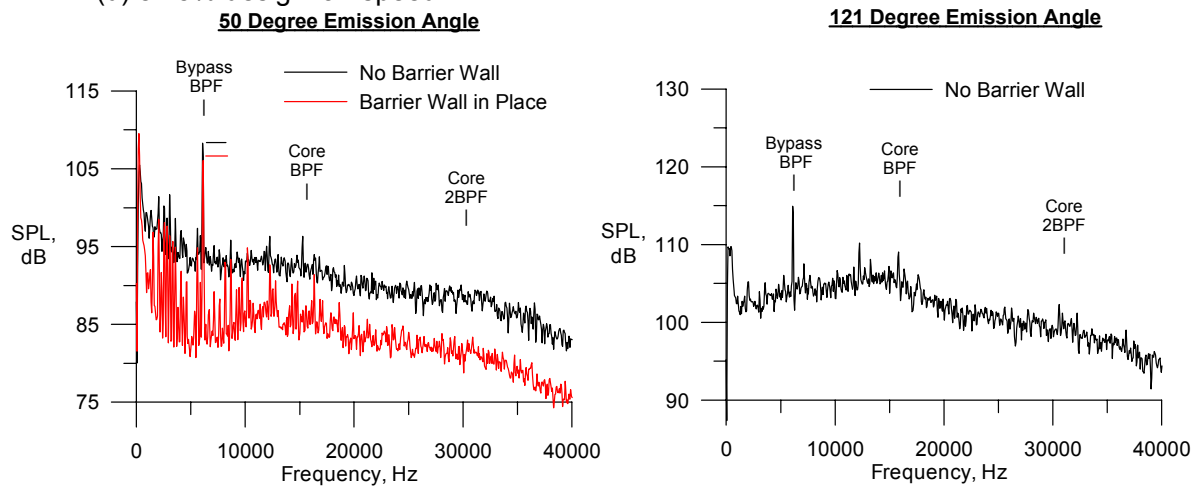

(e) 100% design fan speed

Figure 16.—(Concluded.) Constant (59 Hz) bandwidth sound pressure level spectra (wide chord rotor, baseline stator, lossless data on an 89-in. sideline).

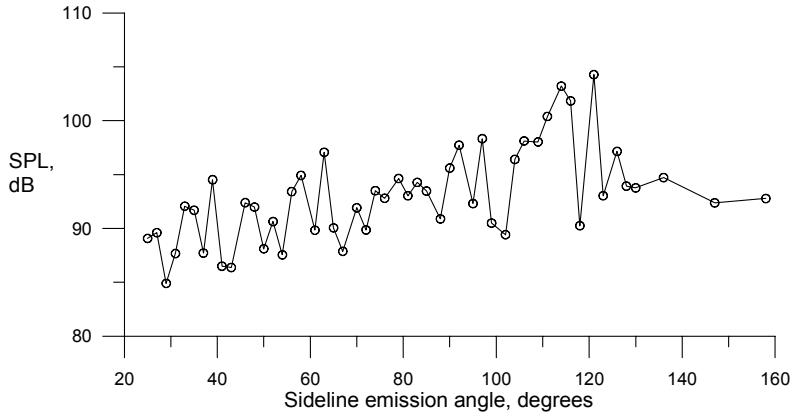

Figure 17.—Constant (59 Hz) bandwidth directivity for the core BPF tone (wide chord rotor, baseline stator, lossless data on 89-in. sideline, fan operating at 61.8 percent).

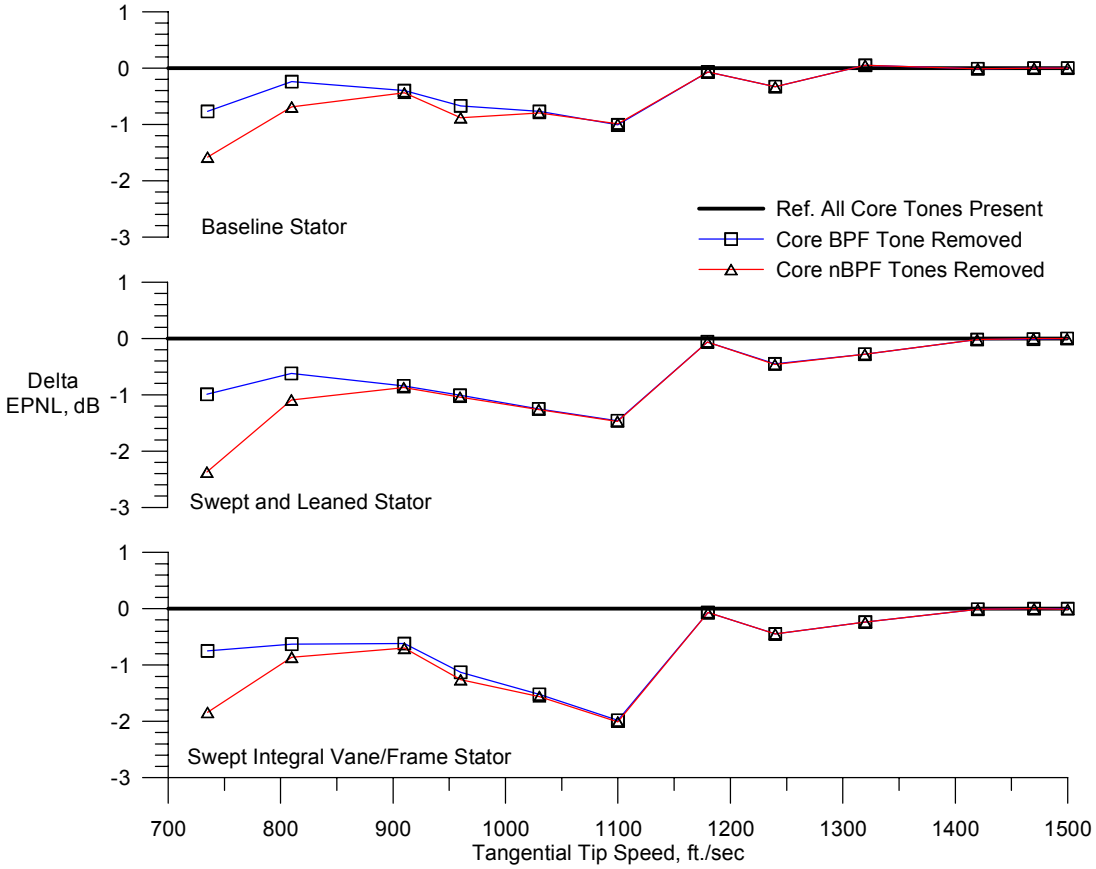

Figure 18.—Effect of removing core rotor tones from EPNL calculations (wide chord rotor, no barrier wall).

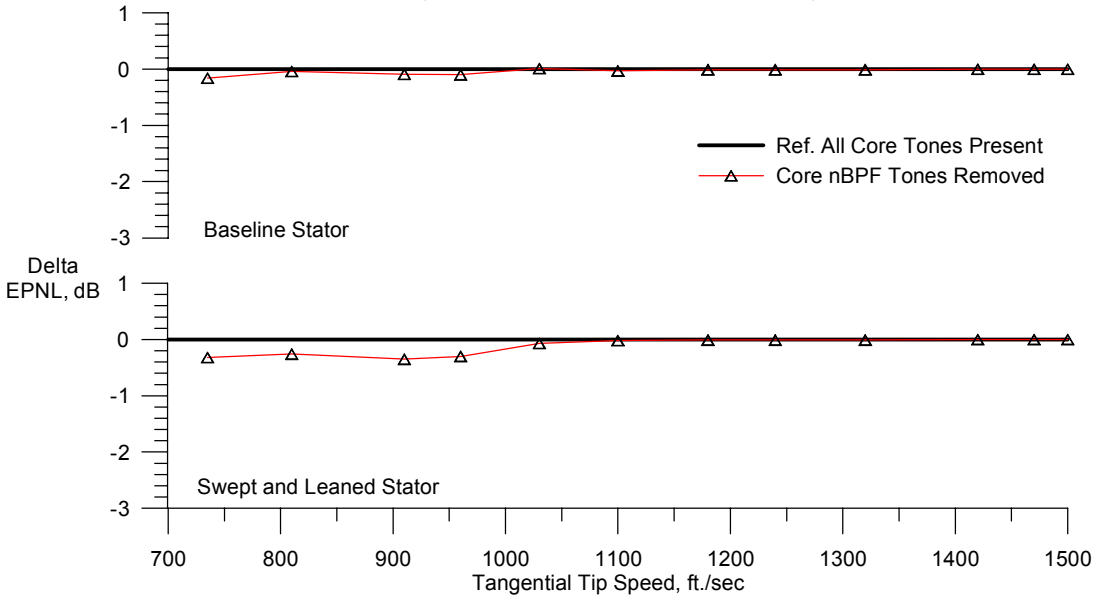

Figure 19.—Effect of removing core rotor tones from EPNL calculation for inlet—radiating noise (wide chord rotor, barrier wall in place).

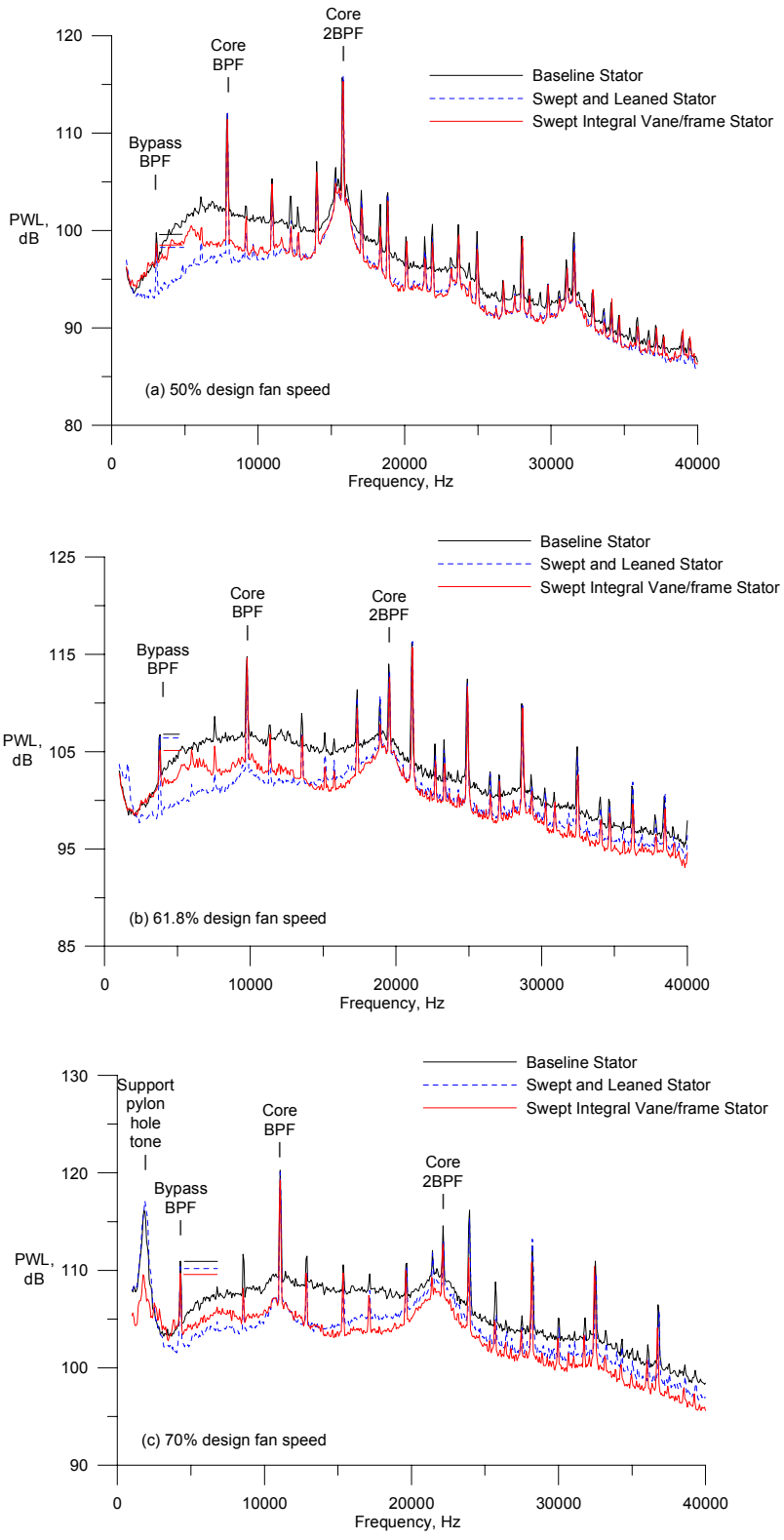

Figure 20.—Sound power level spectra for the wide chord rotor and three stators sets (59 Hz bandwidth).

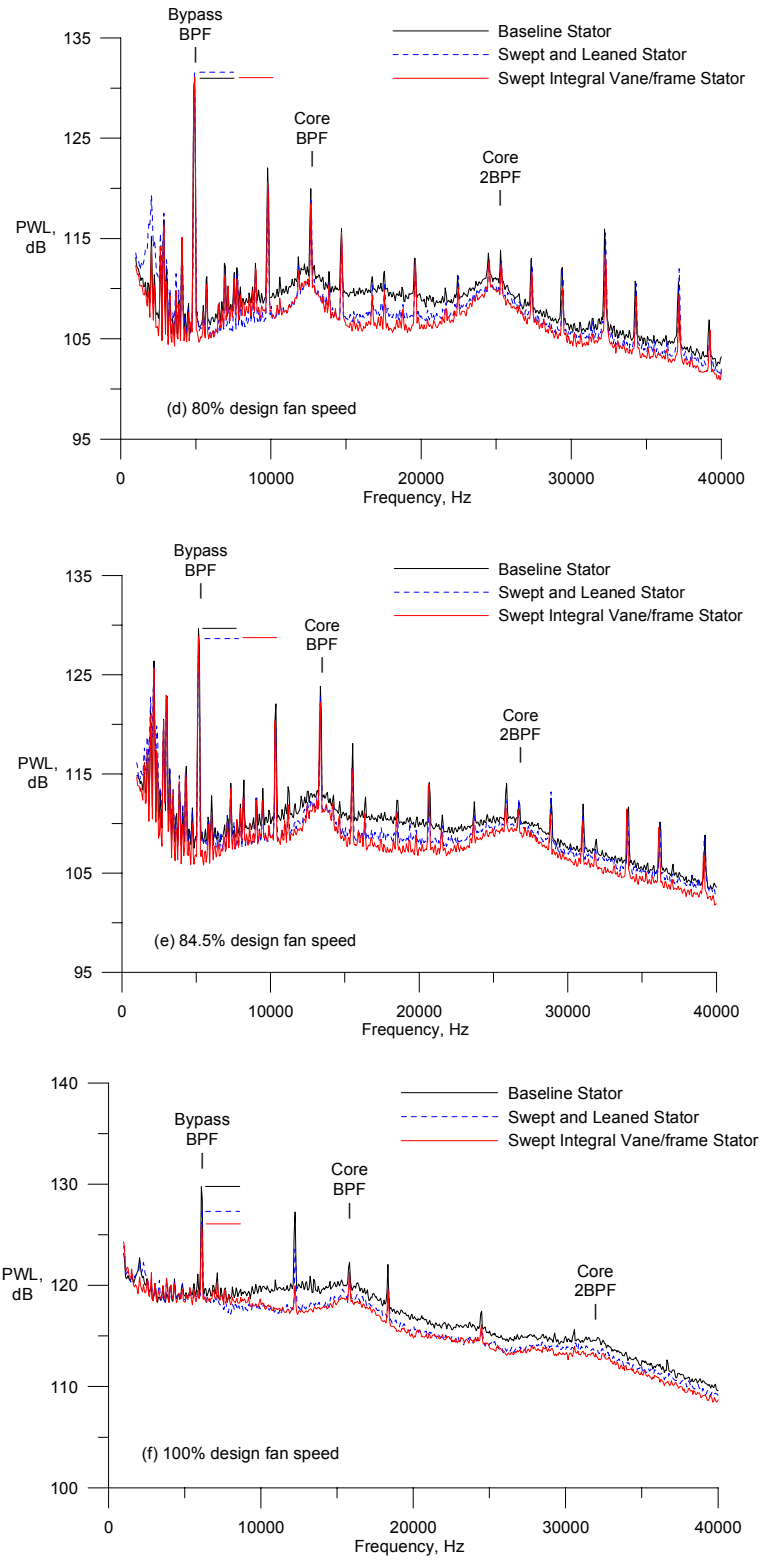

Figure 20.—(Concluded.) Sound power level spectra for the wide chord rotor and three stators sets (59 Hz bandwidth).

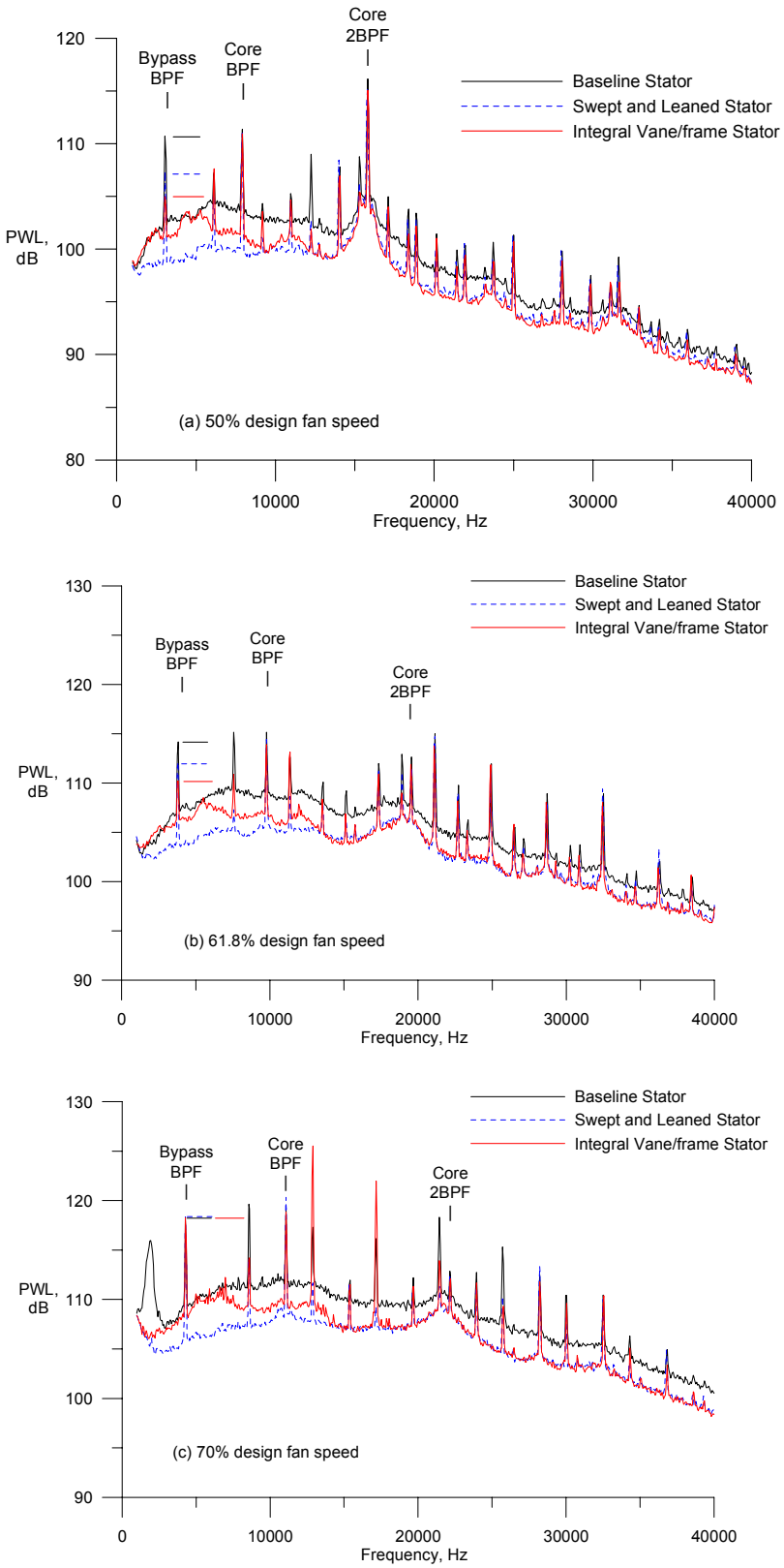

Figure 21.—Sound power level spectra for the forward swept rotor and three stators sets (59 Hz bandwidth).

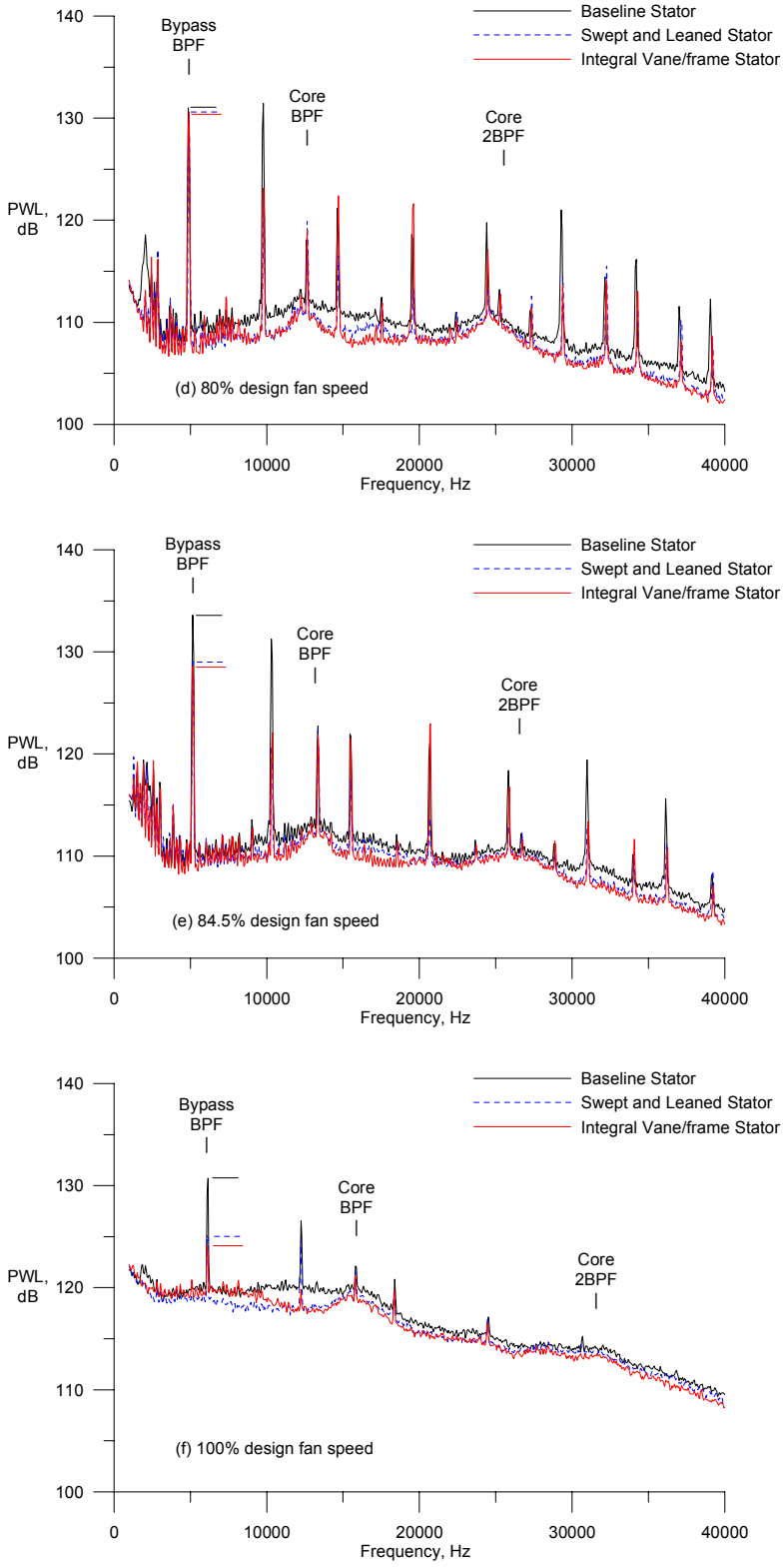

Figure 21.—(Concluded.) Sound power level spectra for the forward swept rotor and three stators sets. (59 Hz bandwidth)

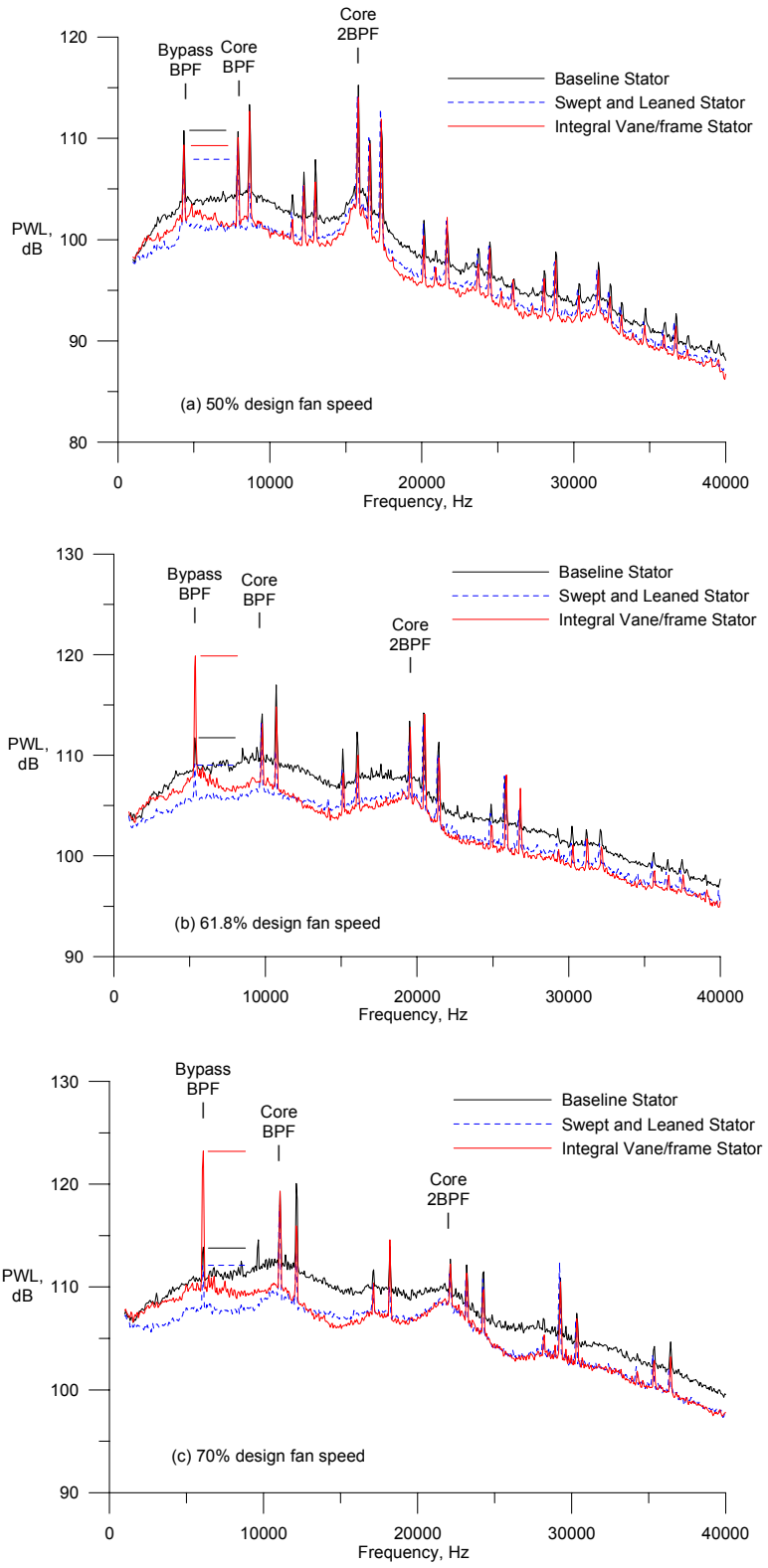

Figure 22.—Sound power level spectra for the shrouded rotor and three stators sets. (59 Hz bandwidth)

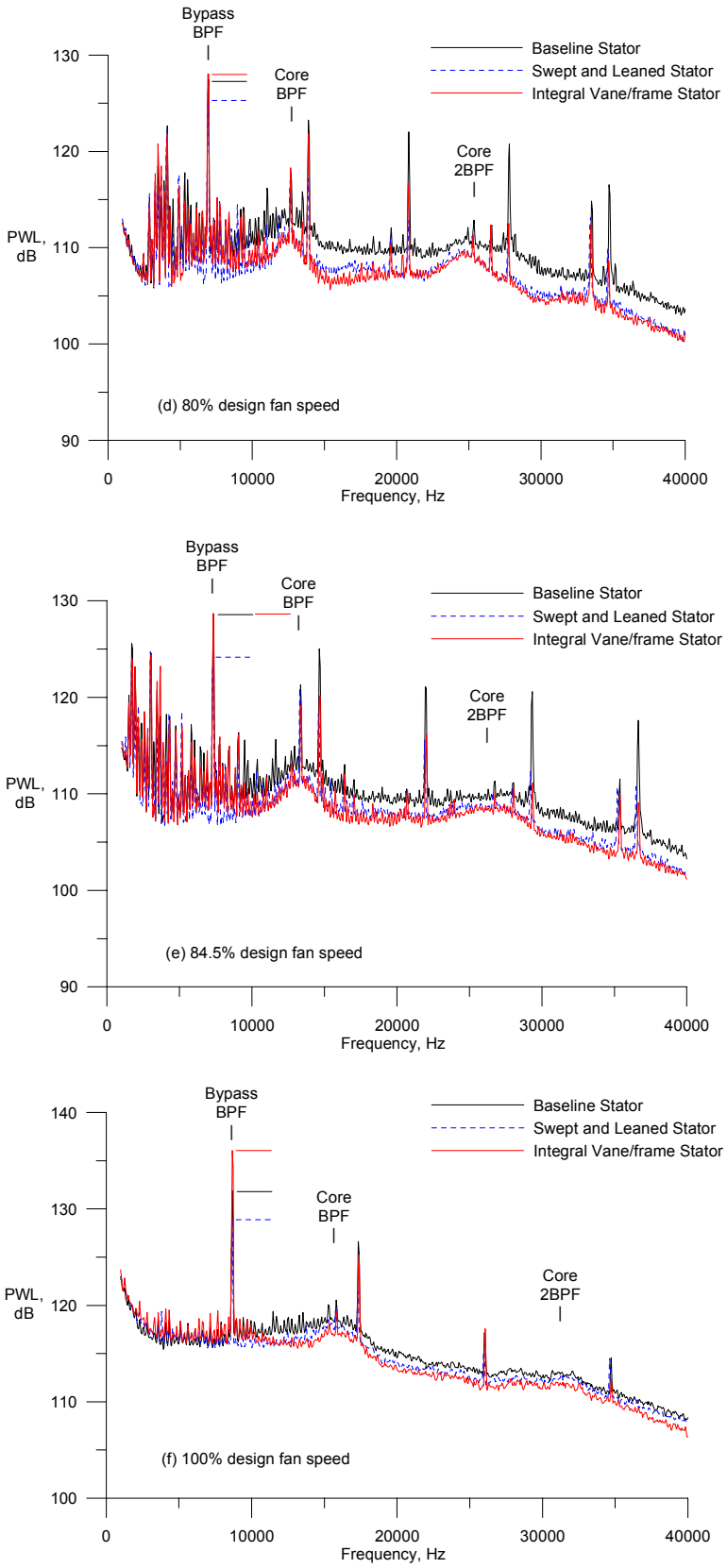

Figure 22.—(Concluded.) Sound power level spectra for the shrouded rotor and three stators sets. (59 Hz bandwidth)

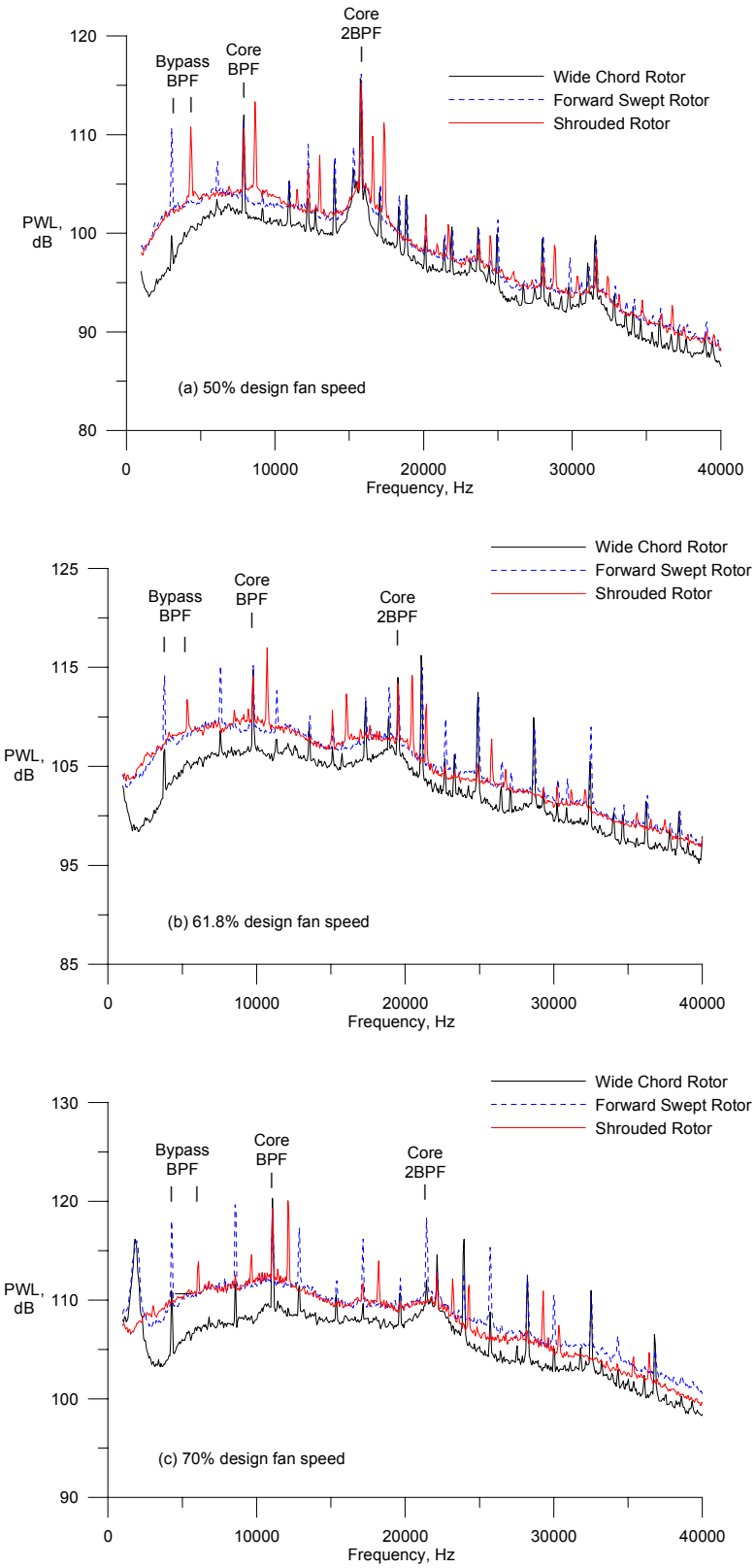

Figure 23.—Sound power level spectra for the baseline stator and three rotors (59 Hz bandwidth).

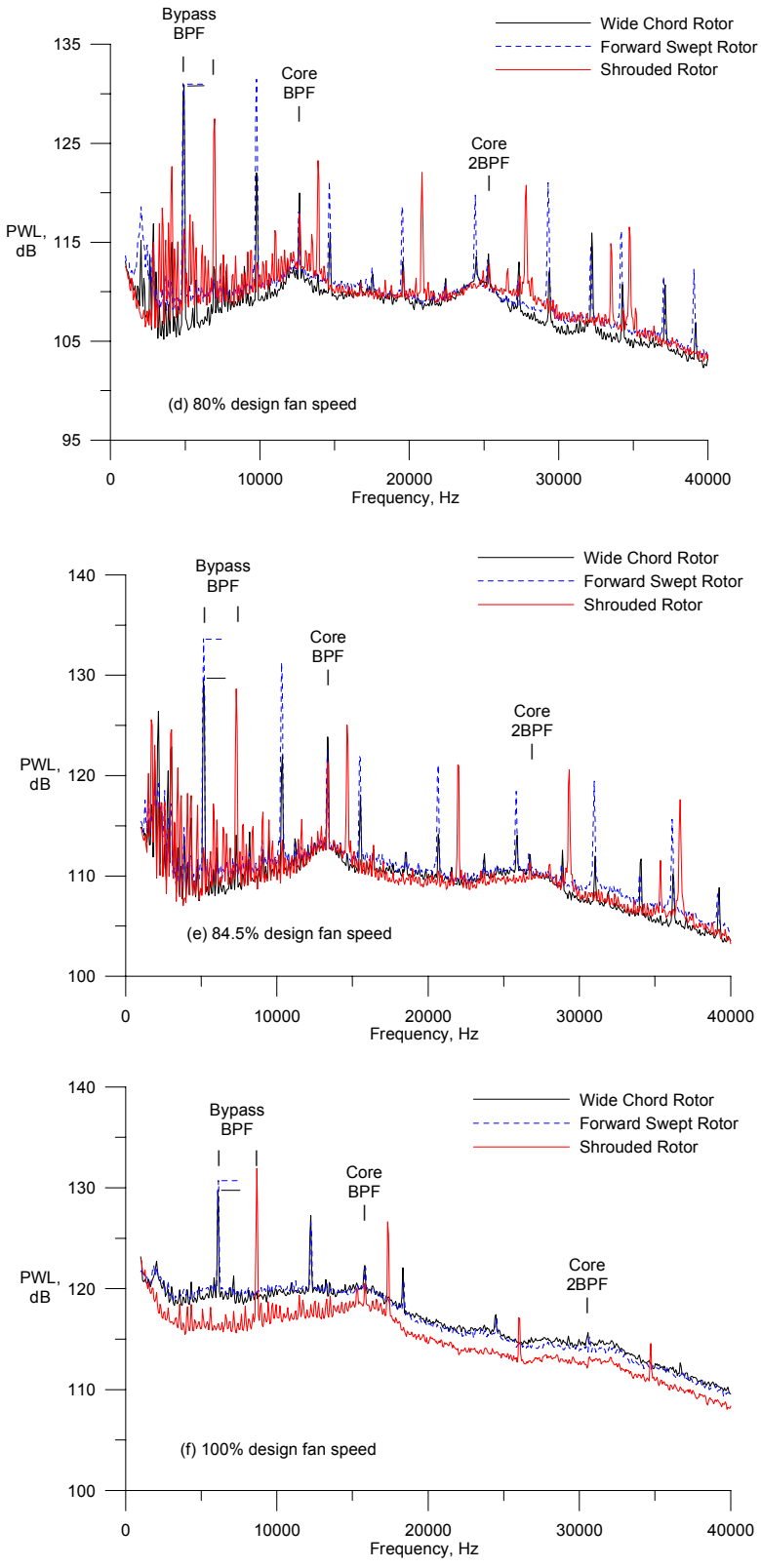

Figure 23.—(Concluded.) Sound power level spectra for the baseline stator and three rotors (59 Hz bandwidth).

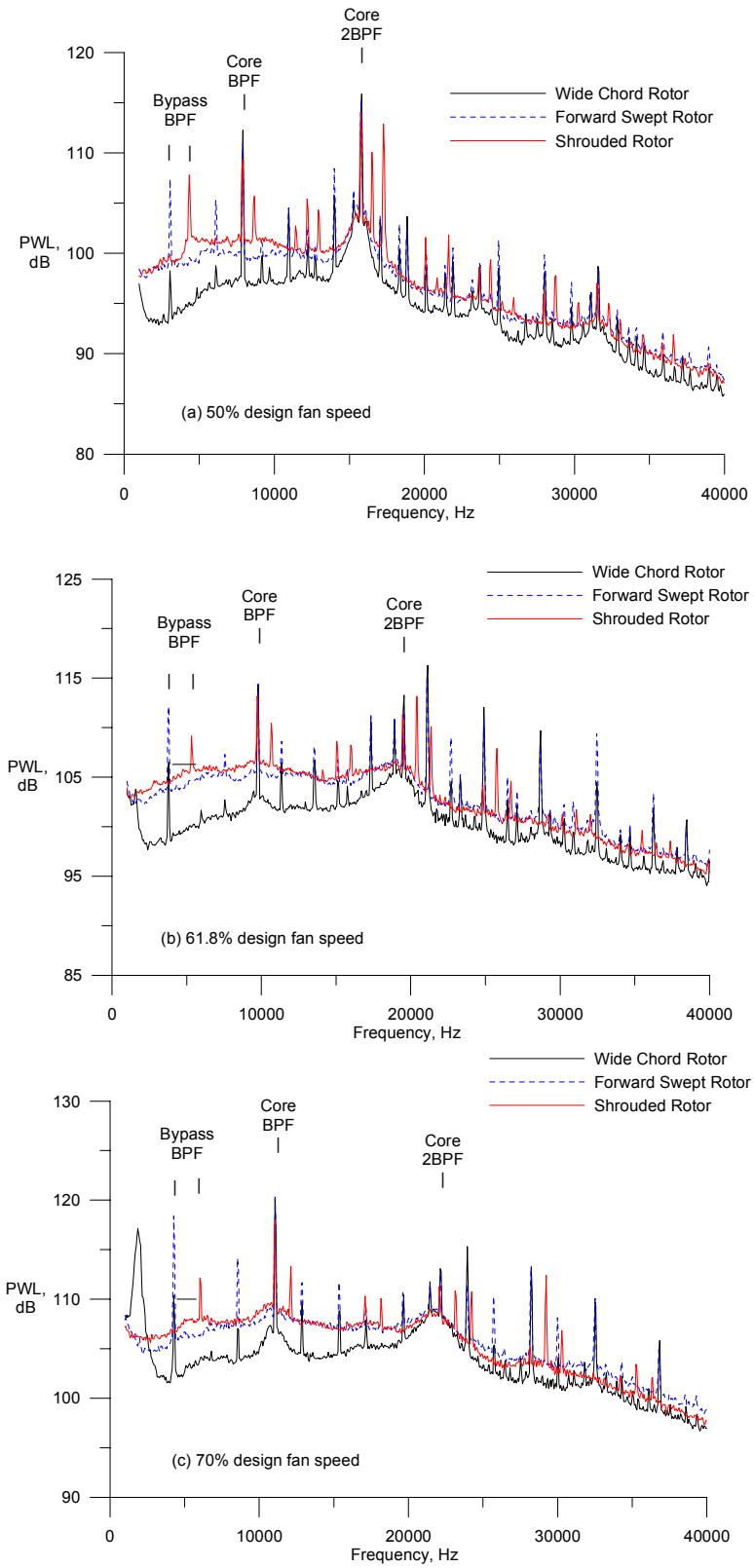

Figure 24.—Sound power level spectra for swept and leaned stator and three rotors (59 Hz bandwidth).

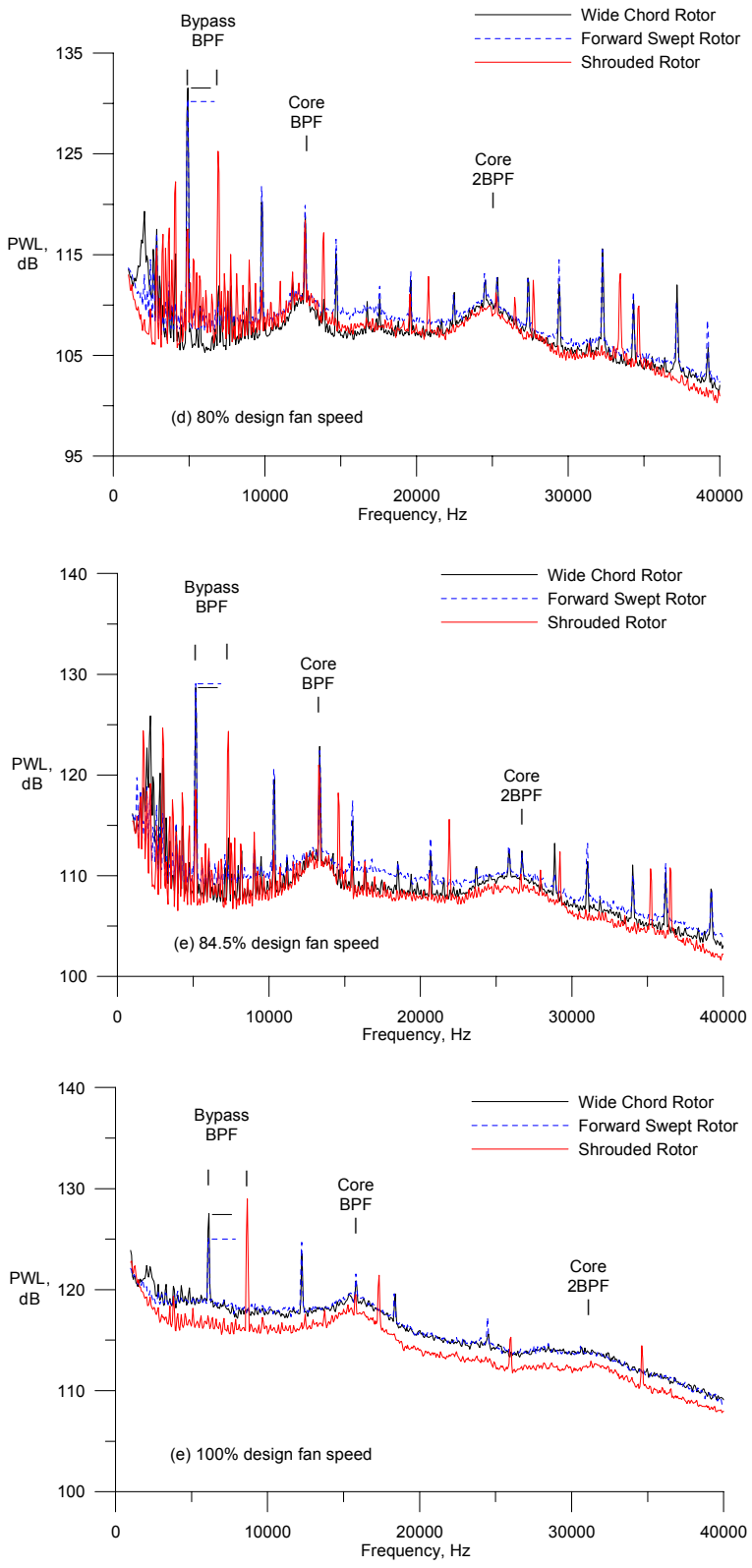

Figure 24.—(Concluded.) Sound power level spectra for swept and leaned stator and three rotors (59 Hz bandwidth).

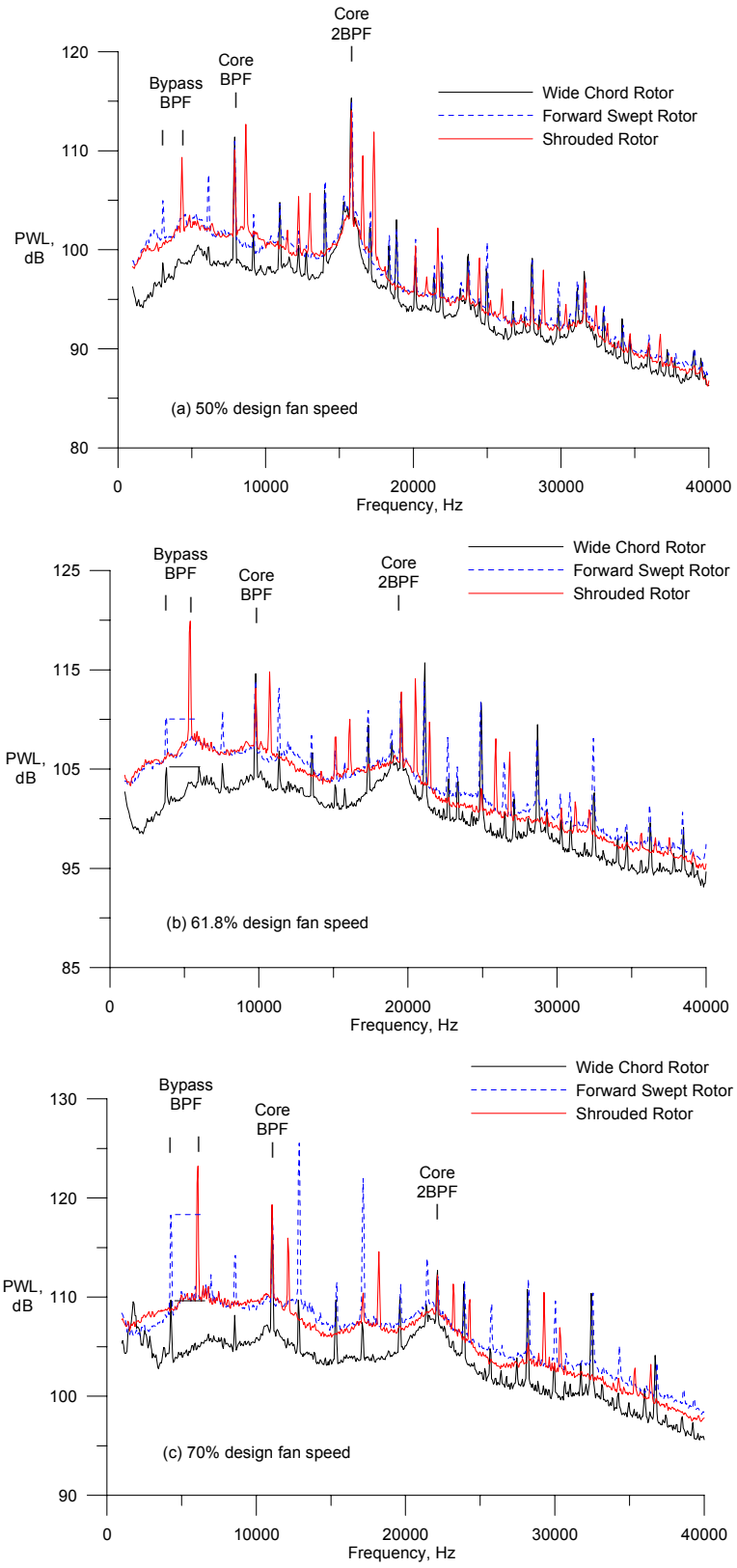

Figure 25.—Sound power level spectra for the integral vane/frame stator and three rotors (59 Hz bandwidth).

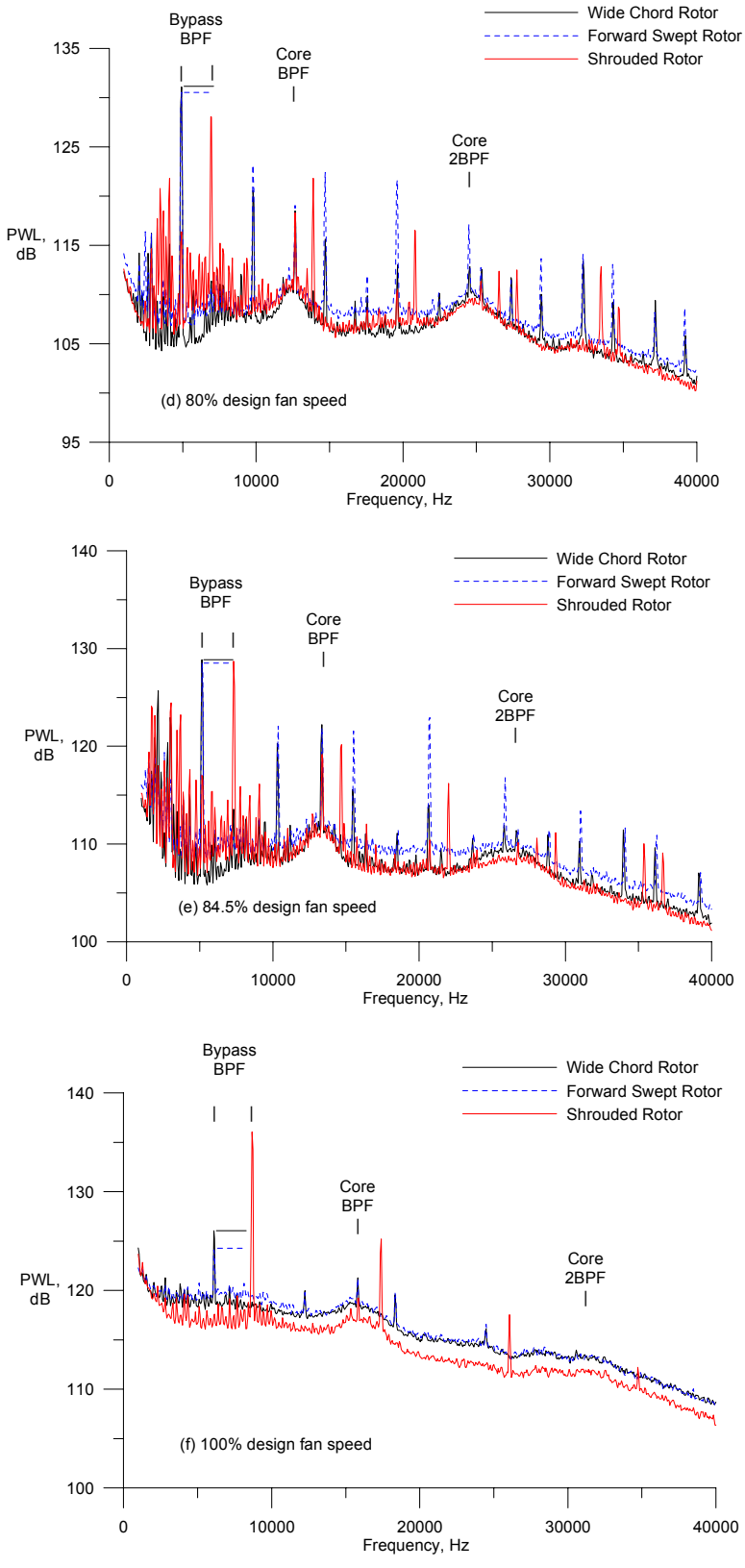

Figure 25.—(Concluded.) Sound power level spectra for the integral vane/frame stator and three rotors (59 Hz bandwidth).

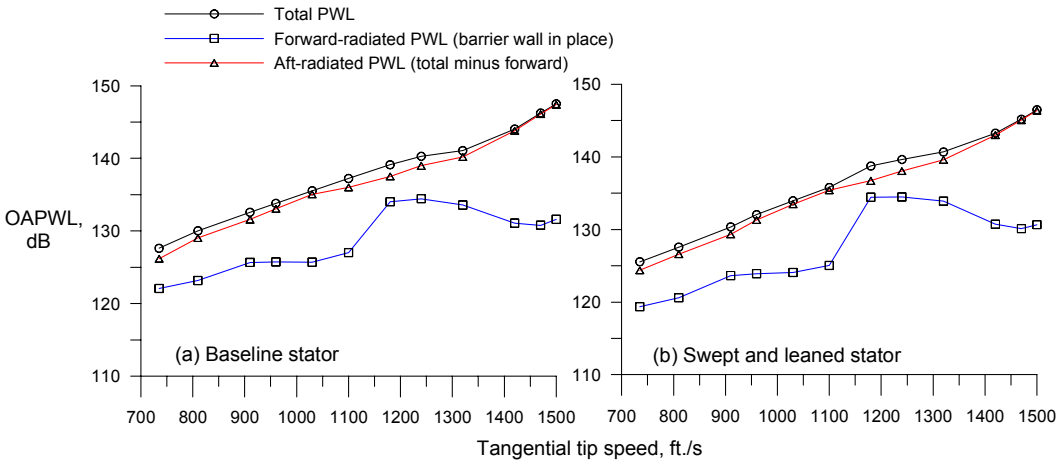

Figure 26.—Overall sound power level forward/aft radiation (wide chord rotor, 2 stator sets, 59Hz bandwidth).

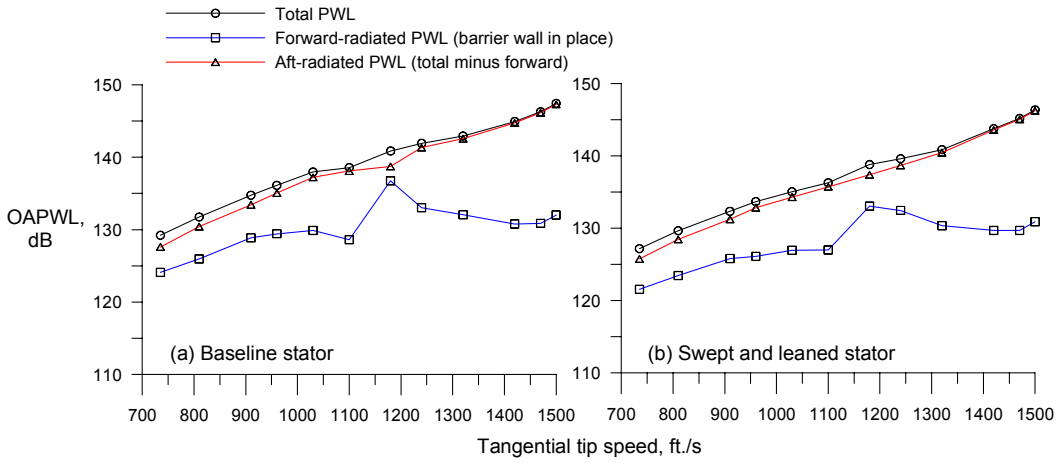

Figure 27.—Overall sound power level forward/aft radiation (forward swept rotor, 2 stator sets, 59 Hz bandwidth).

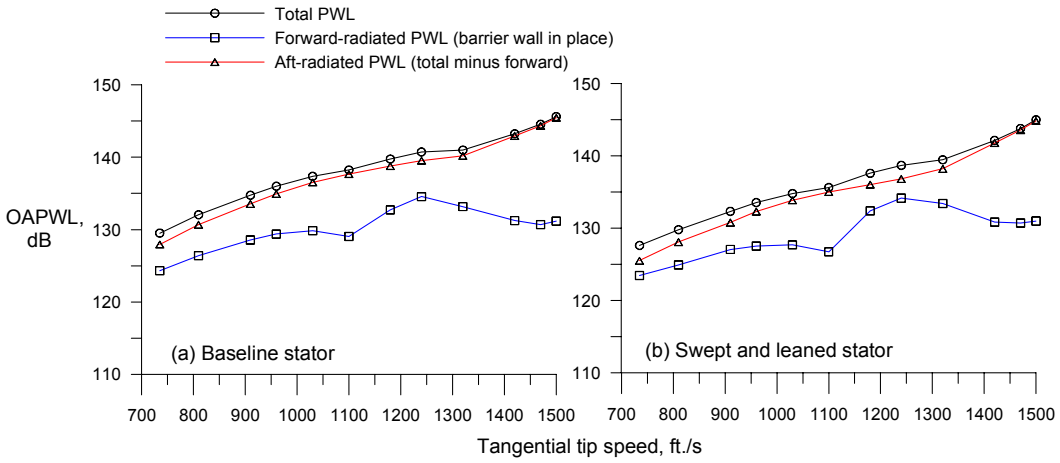

Figure 28.—Overall sound power level forward/aft radiation (shrouded rotor, 2 stator sets, 59 Hz bandwidth).

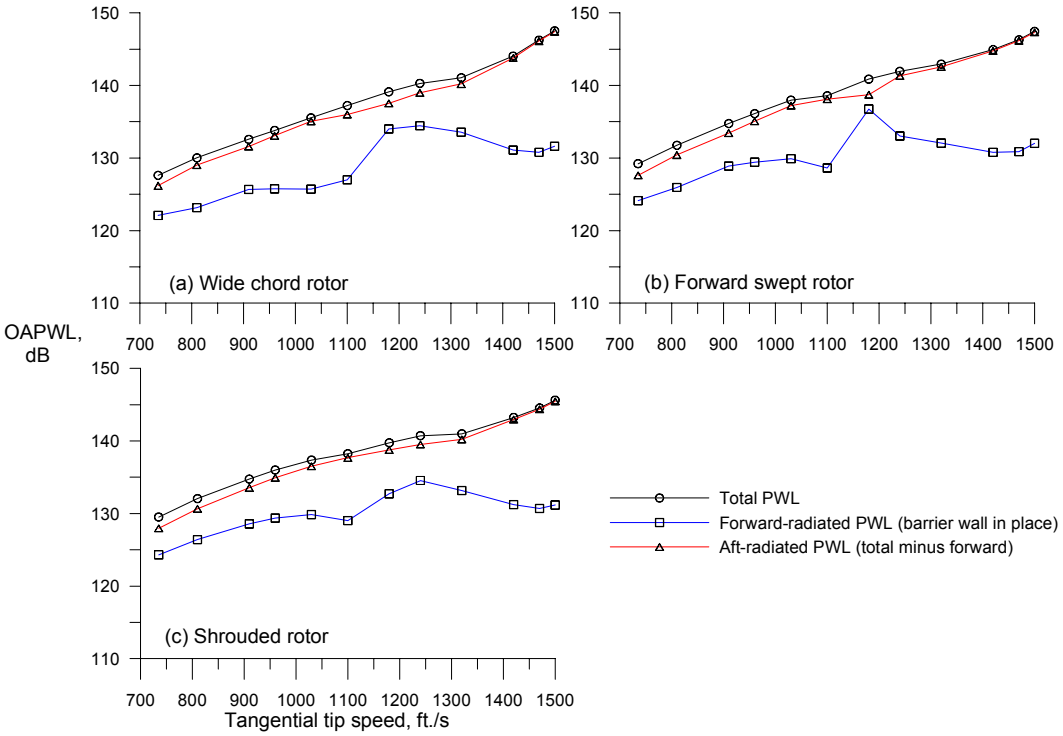

Figure 29.—Overall sound power level forward/aft radiation (baseline stator, 3 rotors, 59 Hz bandwidth).

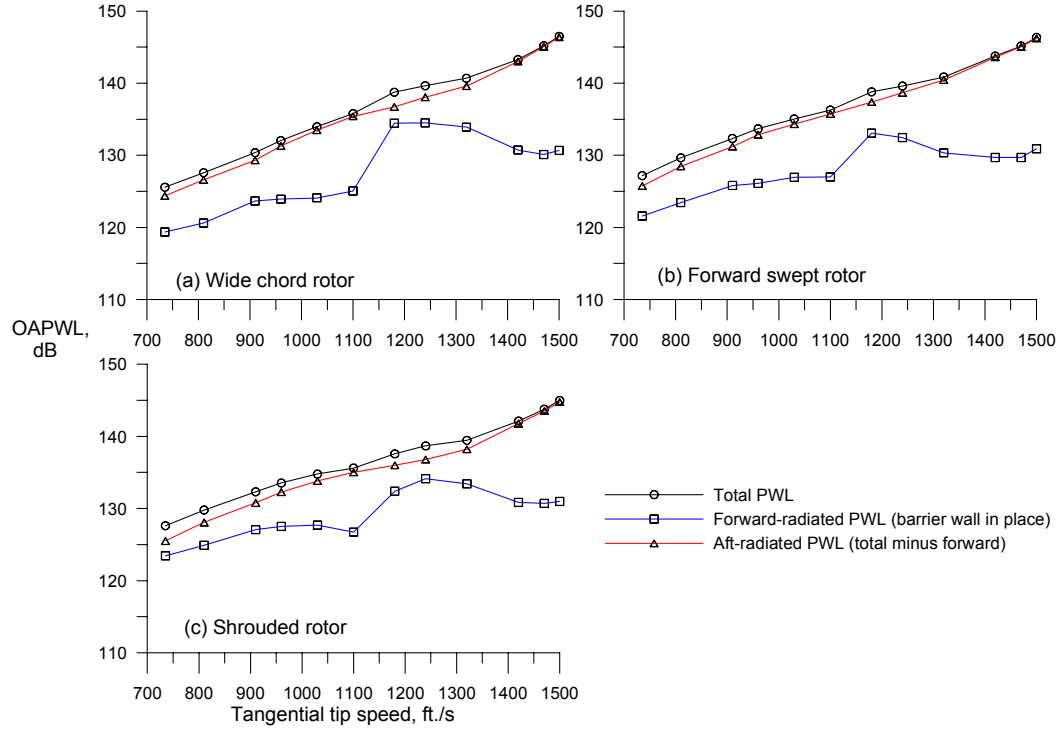

Figure 30.—Overall sound power level forward/aft radiation (swept and leaned stator, 3 rotors, 59 Hz bandwidth).

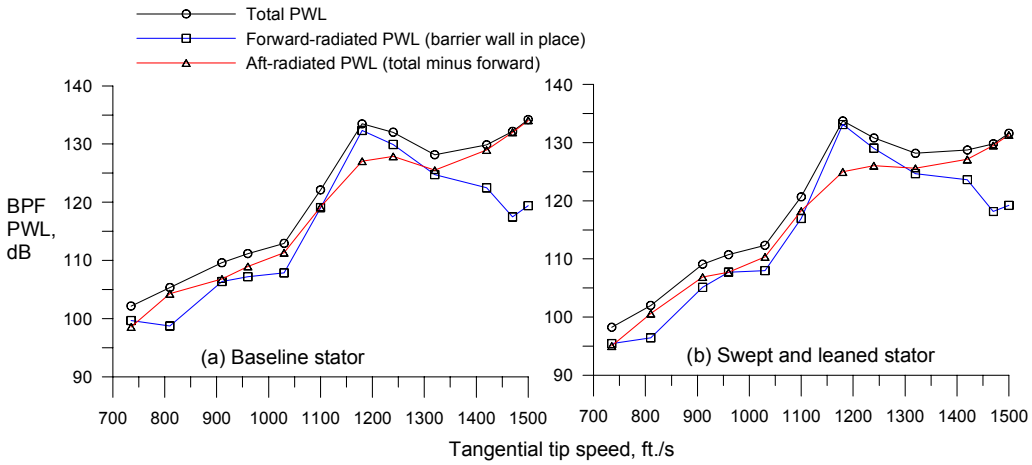

Figure 31.—Blade passage frequency sound power level forward/aft radiation (wide chord rotor, 2 stator sets, 59 Hz bandwidth).

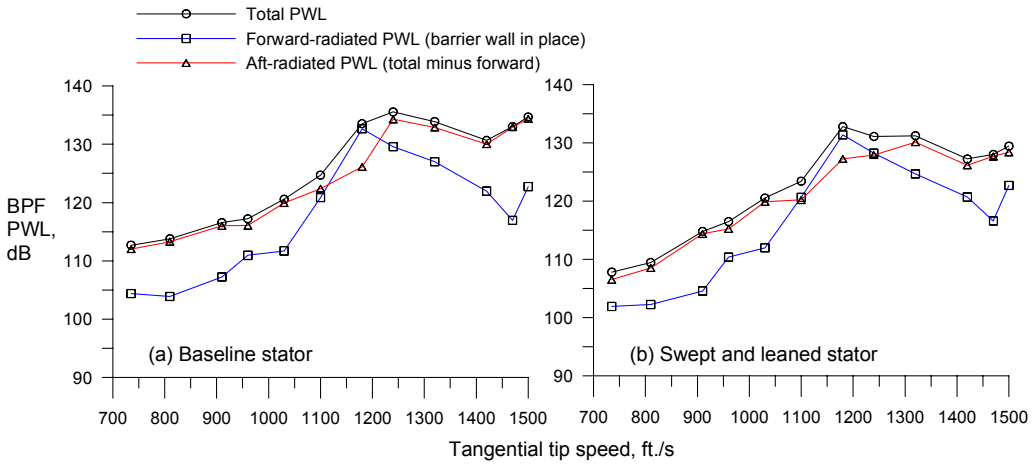

Figure 32.—Blade passage frequency sound power level forward/aft radiation (forward swept rotor, 2 stator sets, 59 Hz bandwidth).

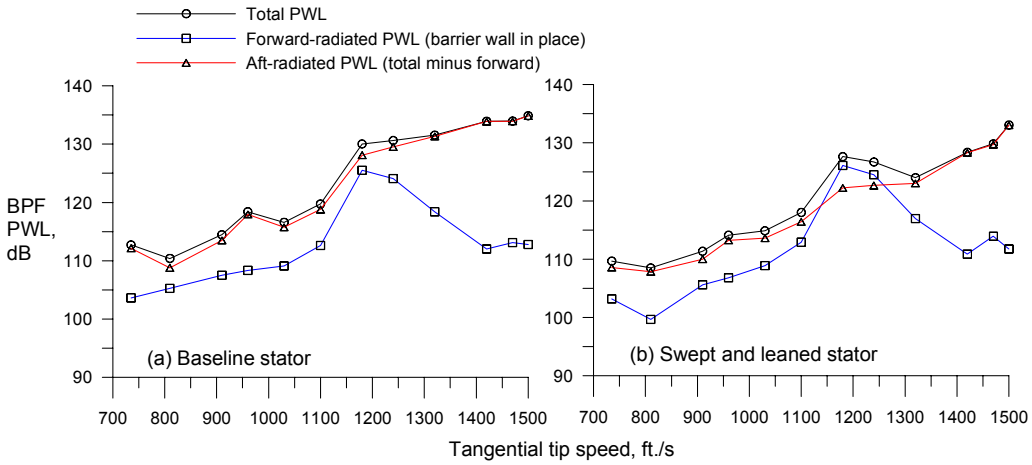

Figure 33.—Blade passage frequency sound power level forward/aft radiation (shrouded rotor, 2 stator sets, 59 Hz bandwidth).

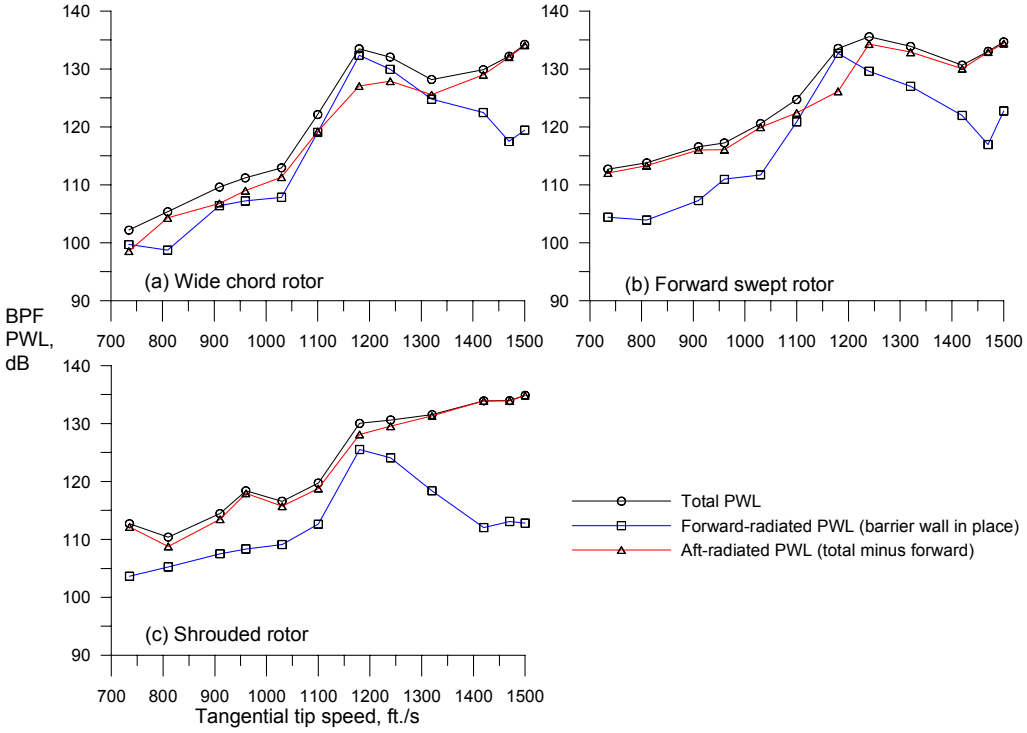

Figure 34.—Blade passage frequency sound power level forward/aft radiation (baseline stator, 3 rotors, 59 Hz bandwidth).

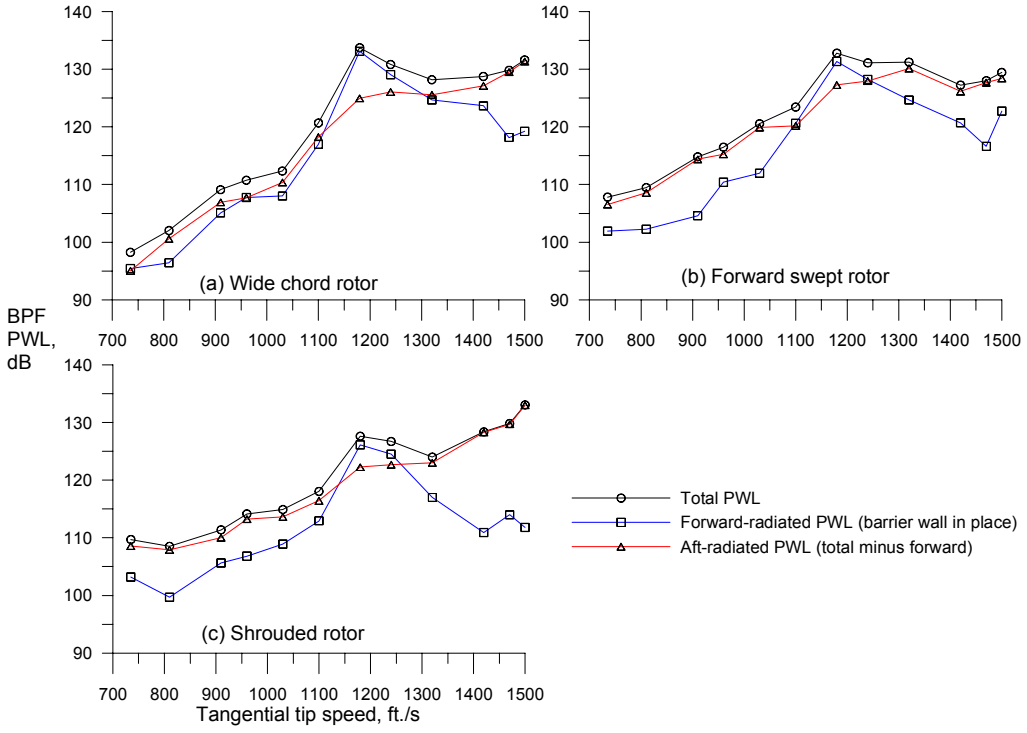

Figure 35.—Blade passage frequency sound power level forward/aft radiation (swept and leaned stator, 3 rotors, 59 Hz bandwidth).

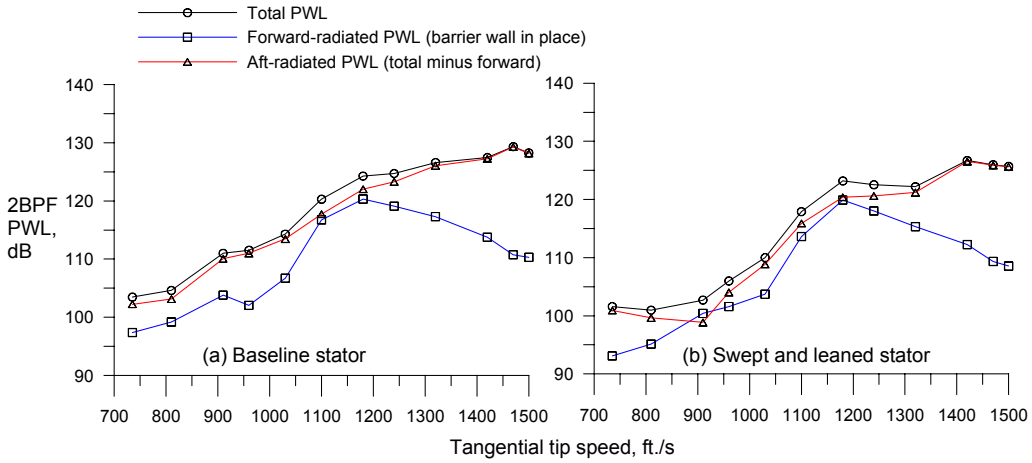

Figure 36.—2xBlade passage frequency sound power level forward/aft radiation (wide chord rotor, 2 stator sets, 59 Hz bandwidth).

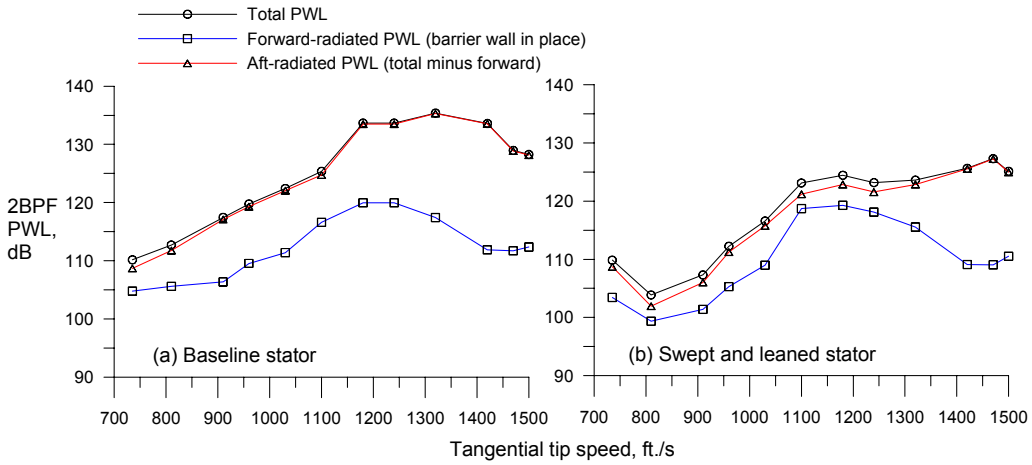

Figure 37.—2xBlade passage frequency sound power level forward/aft radiation (forward swept rotor, 2 stator sets, 59 Hz bandwidth).

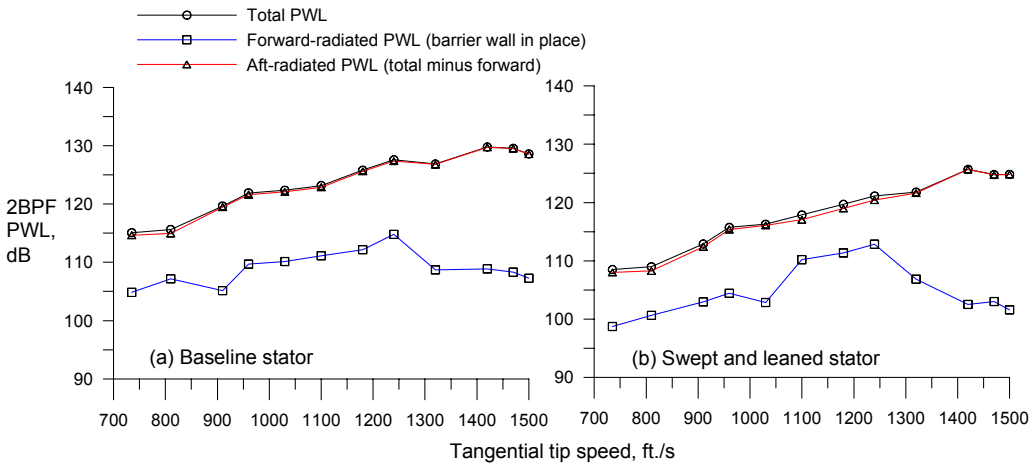

Figure 38.—2xBlade passage frequency sound power level forward/aft radiation (shrouded rotor, 2 stator sets, 59 Hz bandwidth).

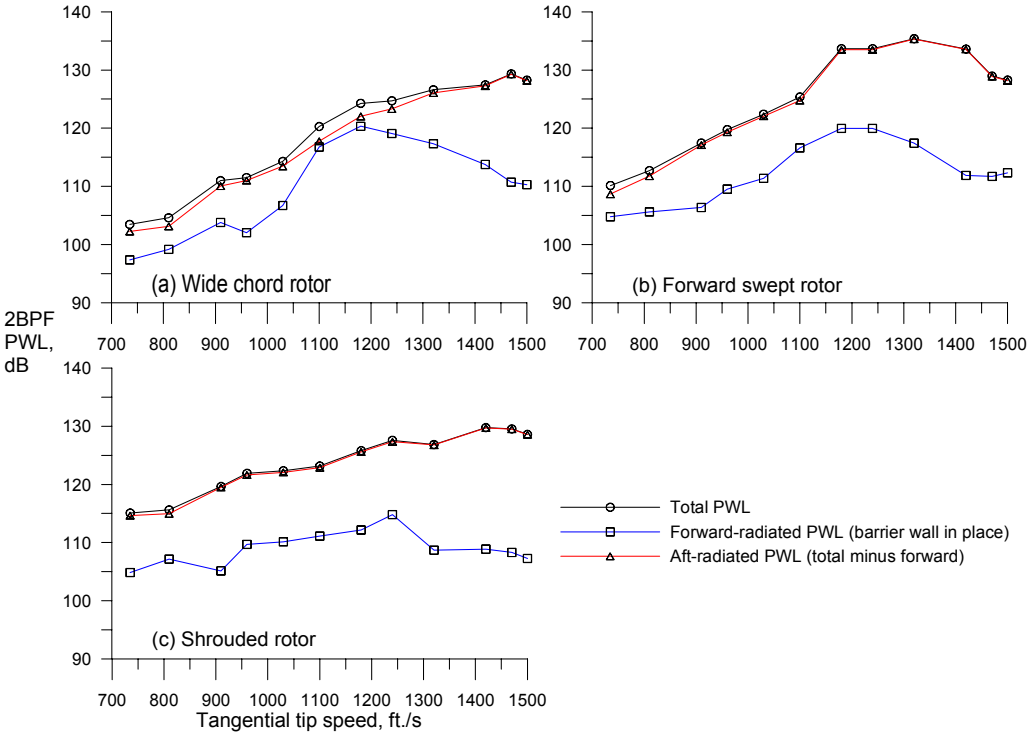

Figure 39.—2xBlade passage frequency sound power level forward/aft radiation (baseline stator, 3 rotors, 59 Hz bandwidth).

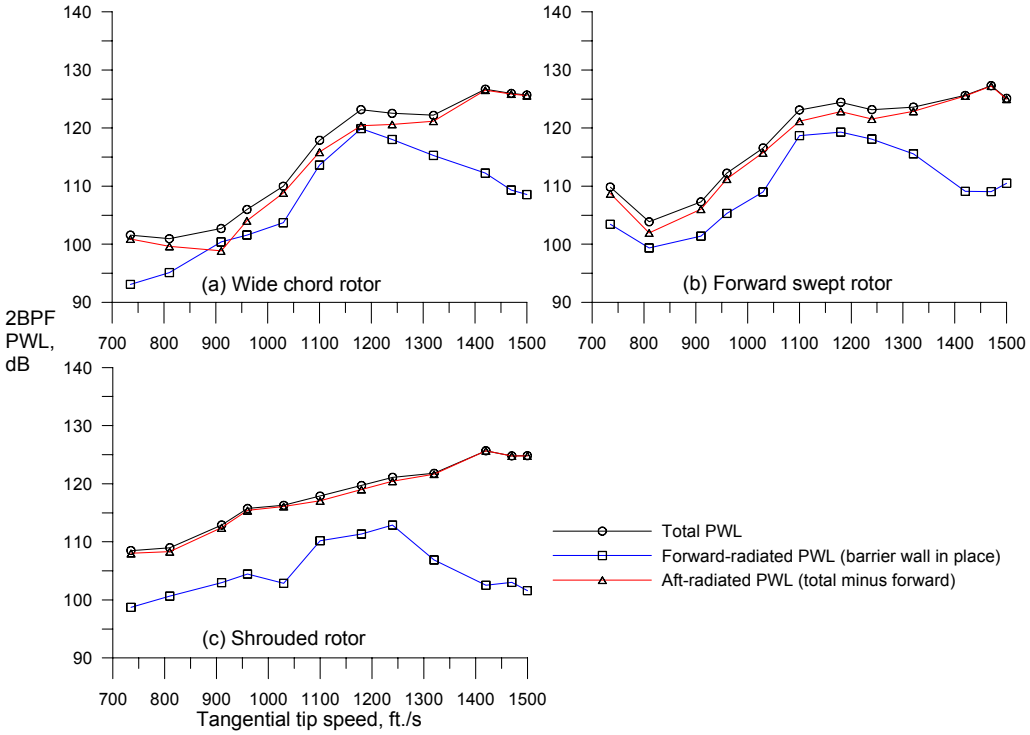

Figure 40.—2xBlade passage frequency sound power level forward/aft radiation (swept and leaned stator, 3 rotors, 59 Hz bandwidth).

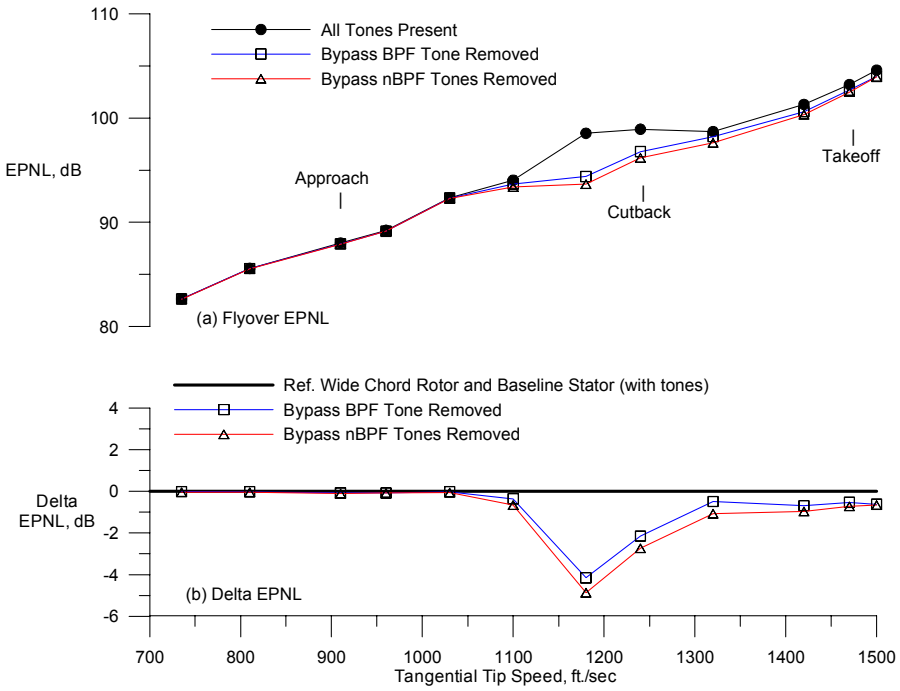

Figure 41.—Flyover EPNL for the wide chord rotor and baseline stator (core rotor tones removed).

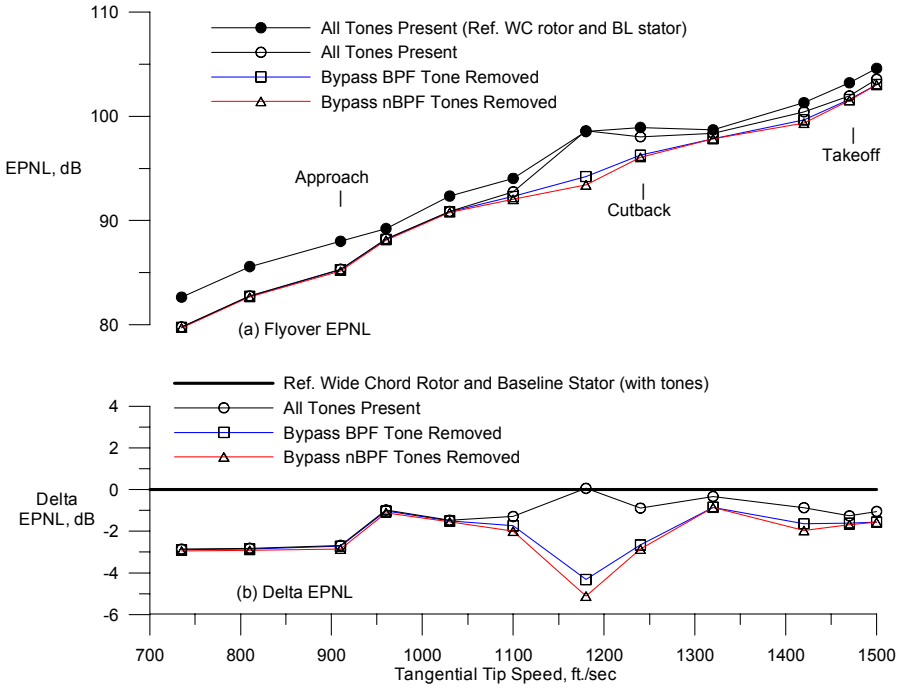

Figure 42.—Flyover EPNL for the wide chord rotor and swept and leaned stator (core rotor tones removed).

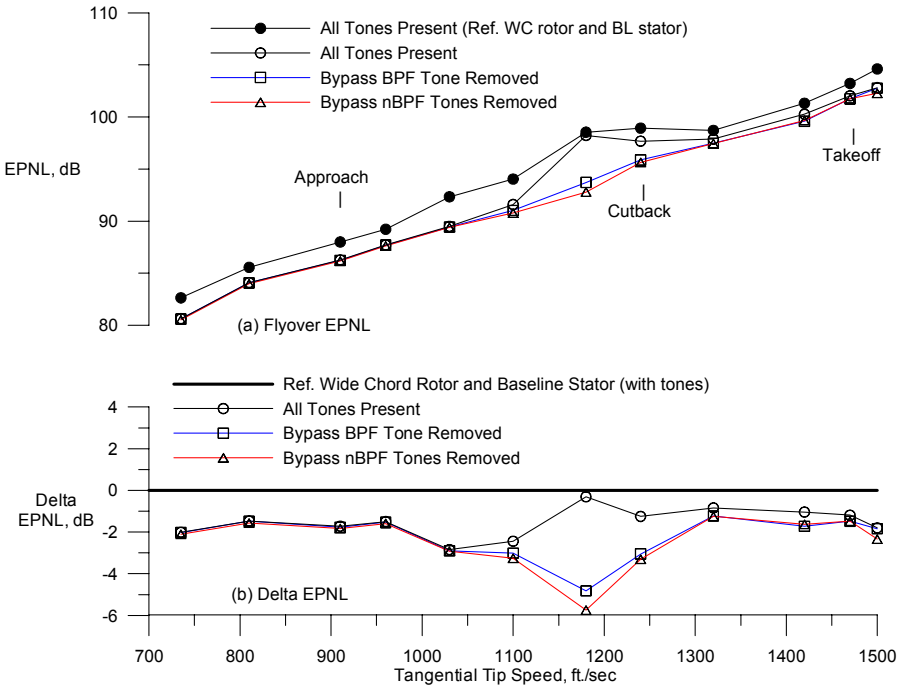

Figure 43.—Flyover EPNL for the wide chord rotor and integral vane/frame stator (core rotor tones removed).

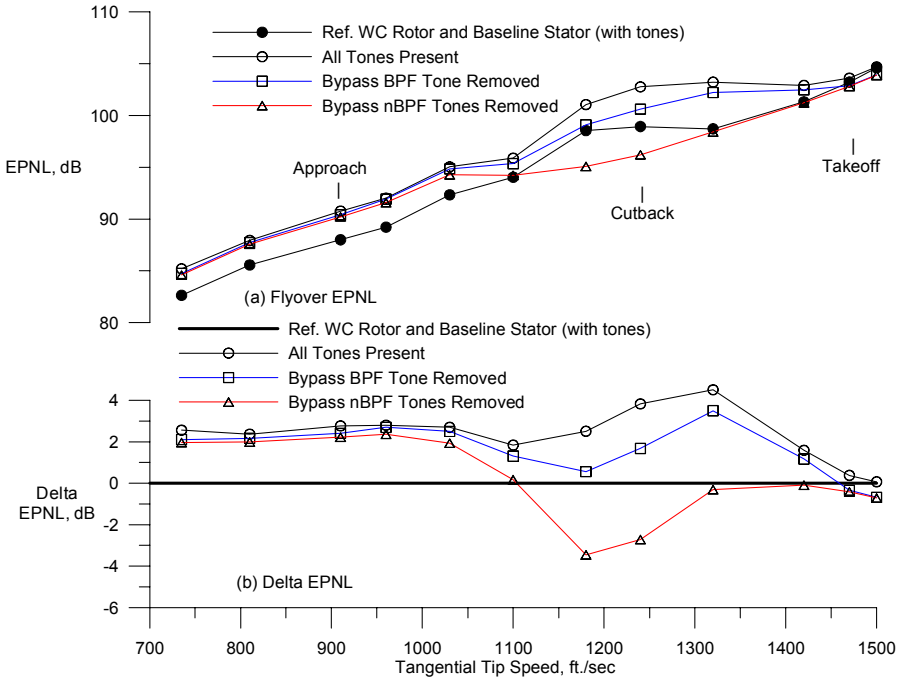

Figure 44.—Flyover EPNL for the forward swept rotor and baseline stator (core rotor tones removed).

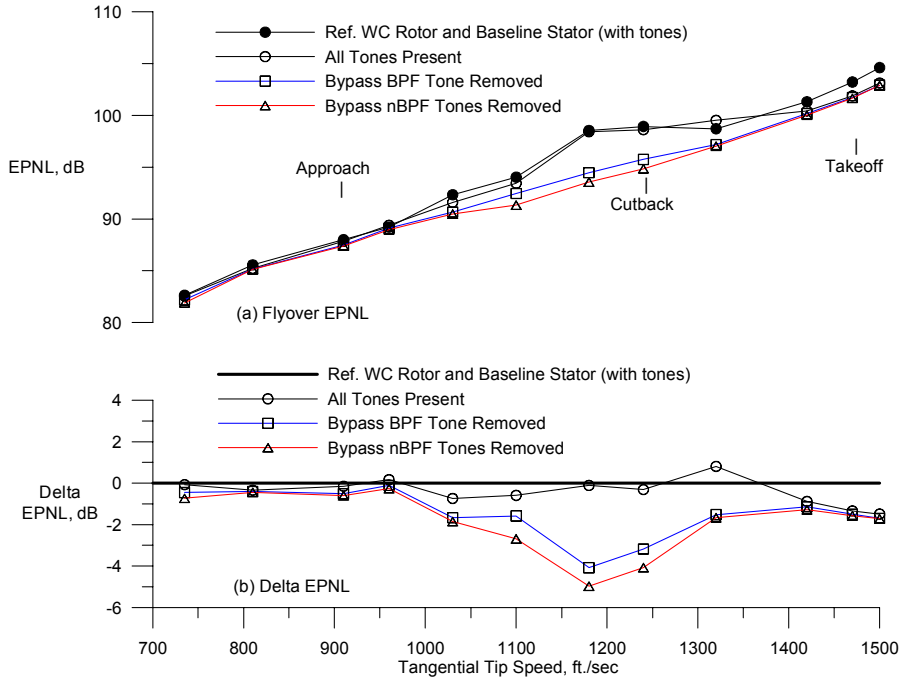

Figure 45.—Flyover EPNL for the forward swept rotor and swept and leaned stator (core rotor tones removed).

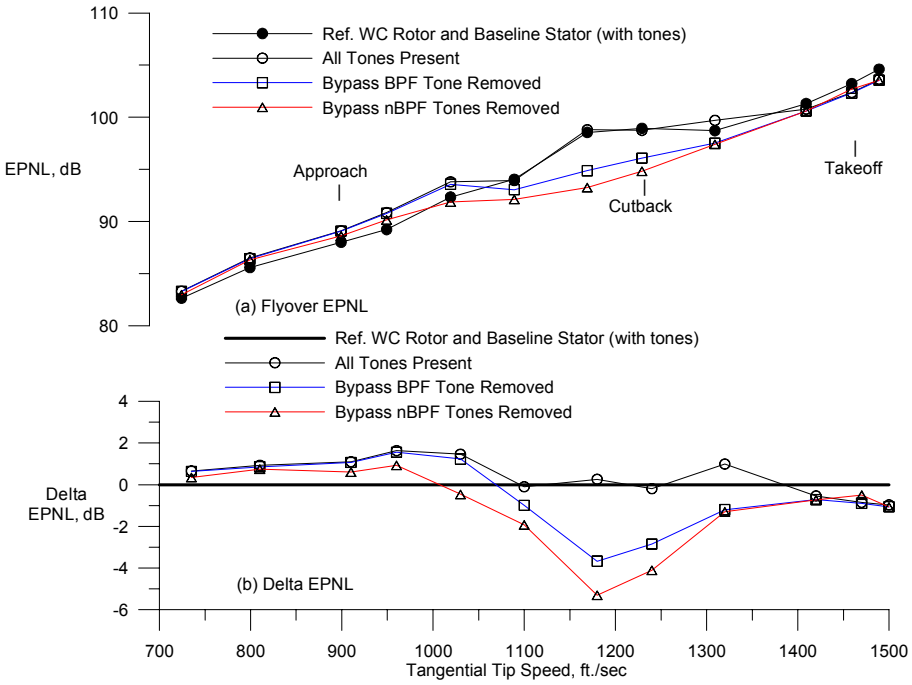

Figure 46.—Flyover EPNL for the forward swept rotor and integral vane/frame stator (core rotor tones removed).

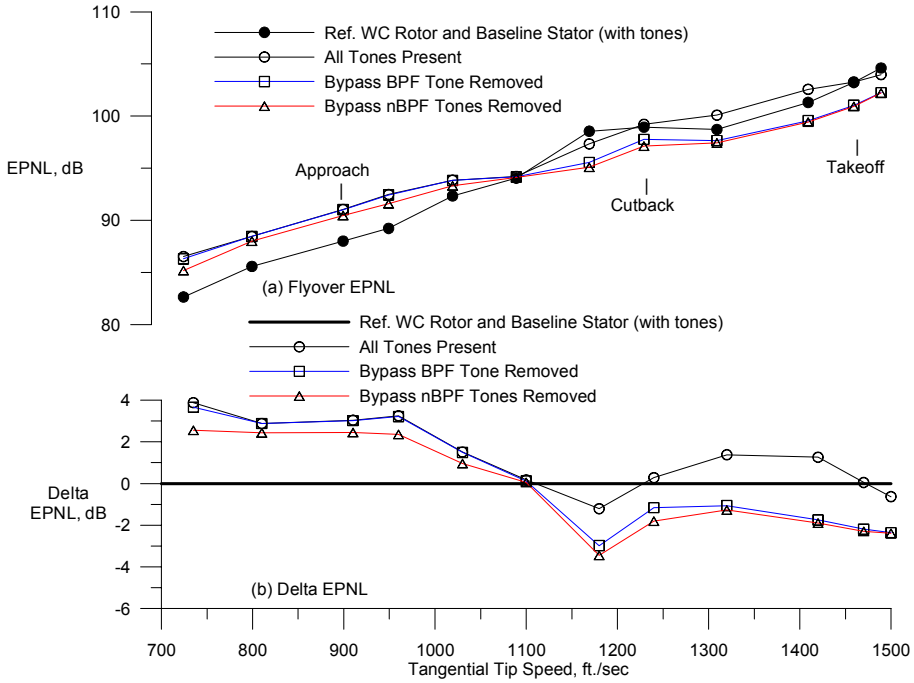

Figure 47.—Flyover EPNL for the shrouded rotor and baseline stator (core rotor tones removed).

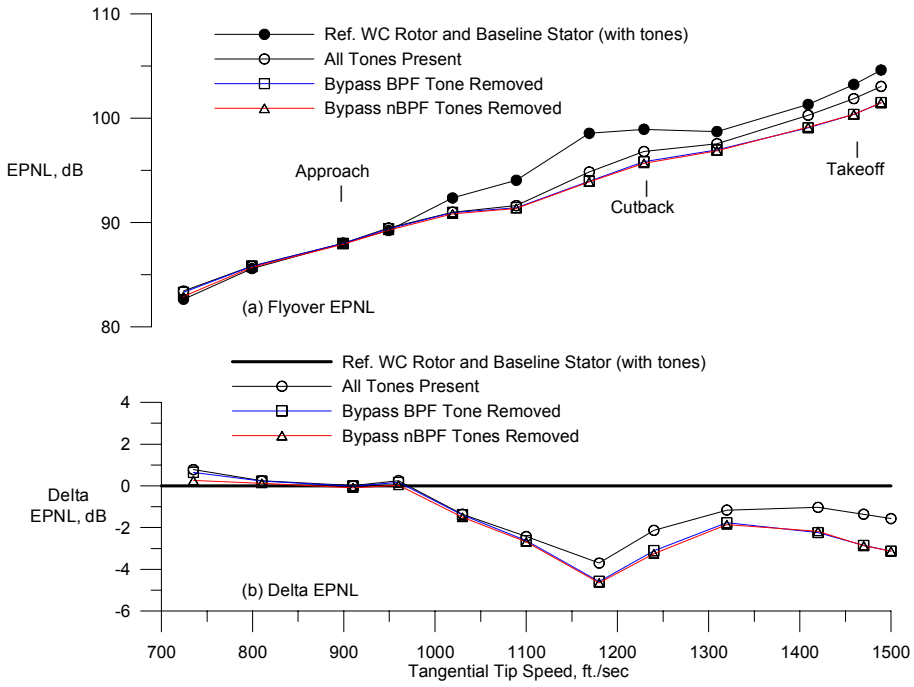

Figure 48.—Flyover EPNL for the shrouded rotor and swept and leaned stator (core rotor tones removed).

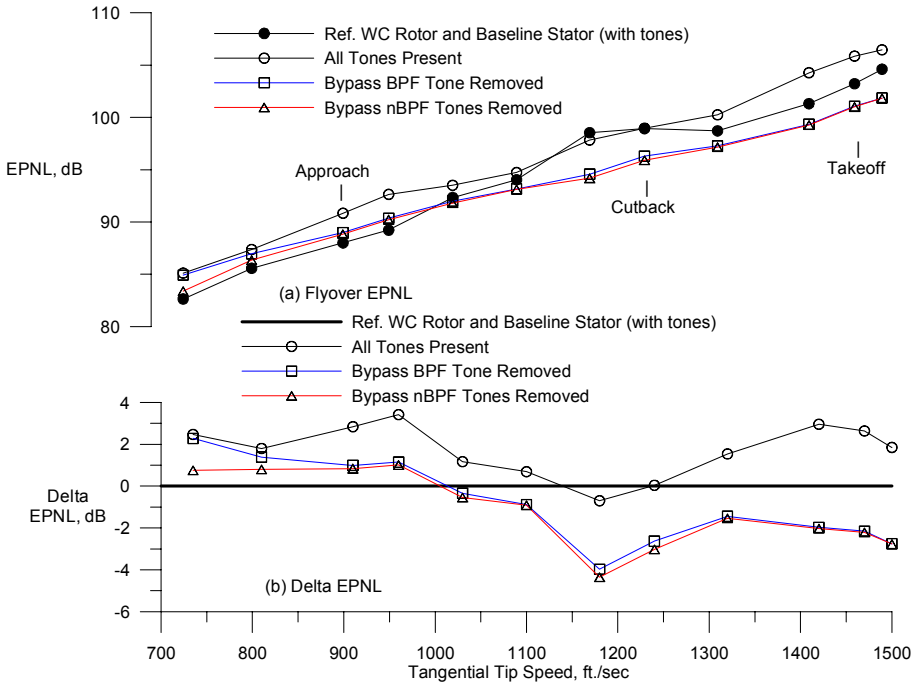

Figure 49.—Flyover EPNL for the shrouded rotor and integral vane/frame stator (core rotor tones removed).

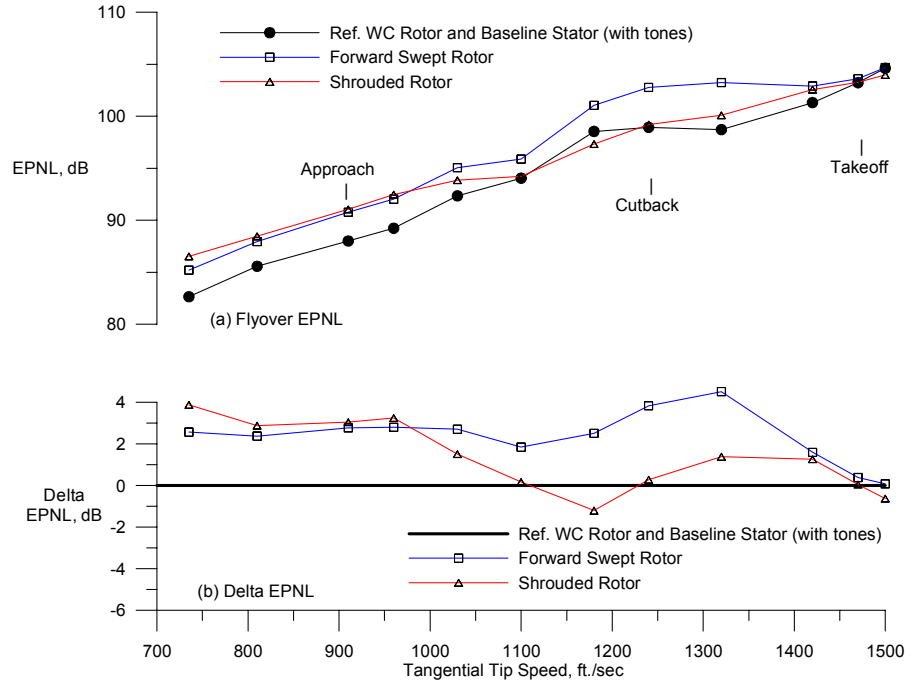

Figure 50.—Flyover EPNL for baseline stator and three rotors with all bypass tones present (core rotor tones removed).

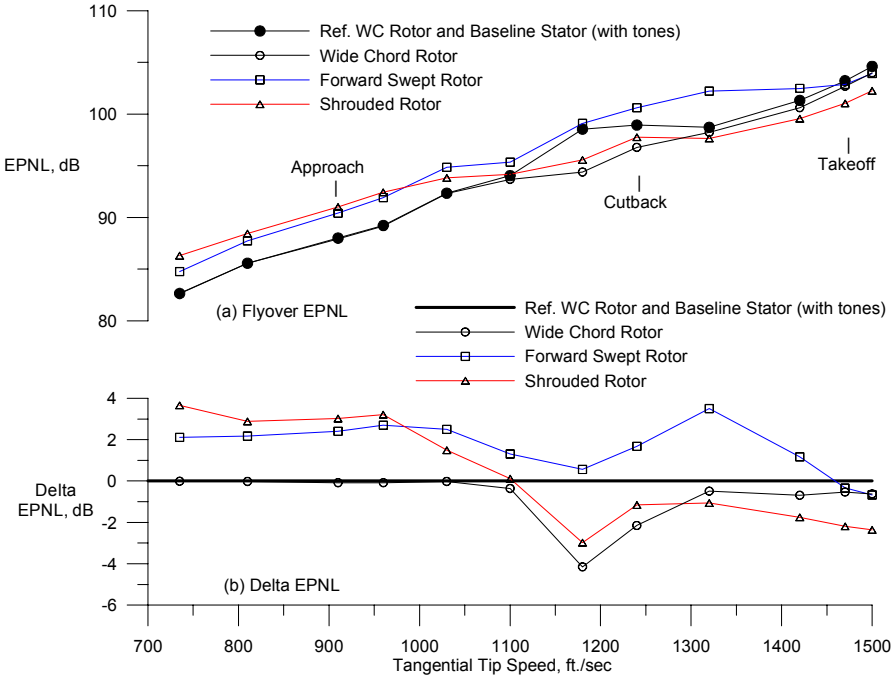

Figure 51.—Flyover EPNL for baseline stator and three rotors with bypass BPF tone removed (core rotor tones removed).

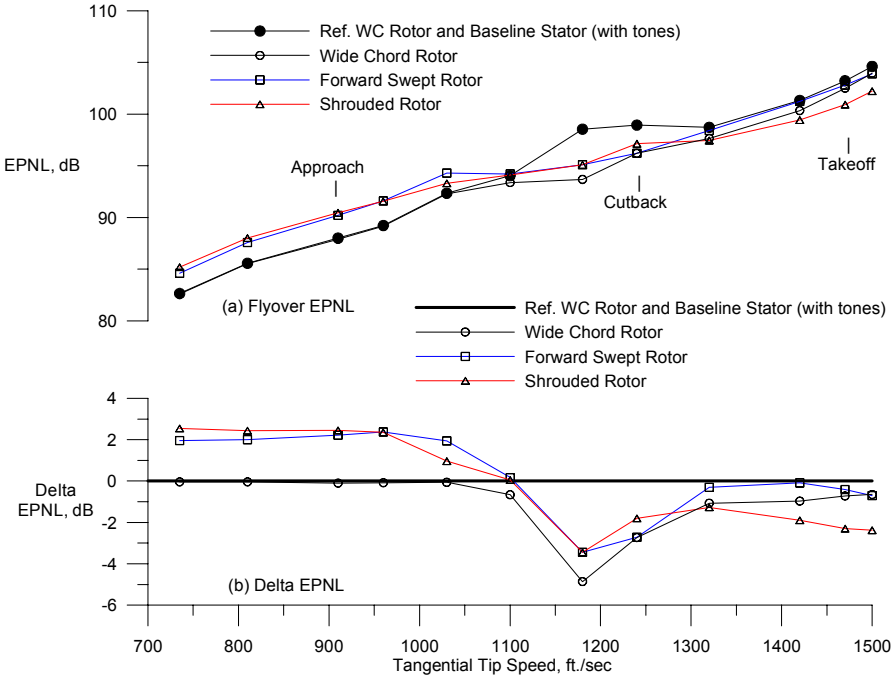

Figure 52.—Flyover EPNL for baseline stator and three rotors with all bypass nBPF tones removed (core rotor tones removed).

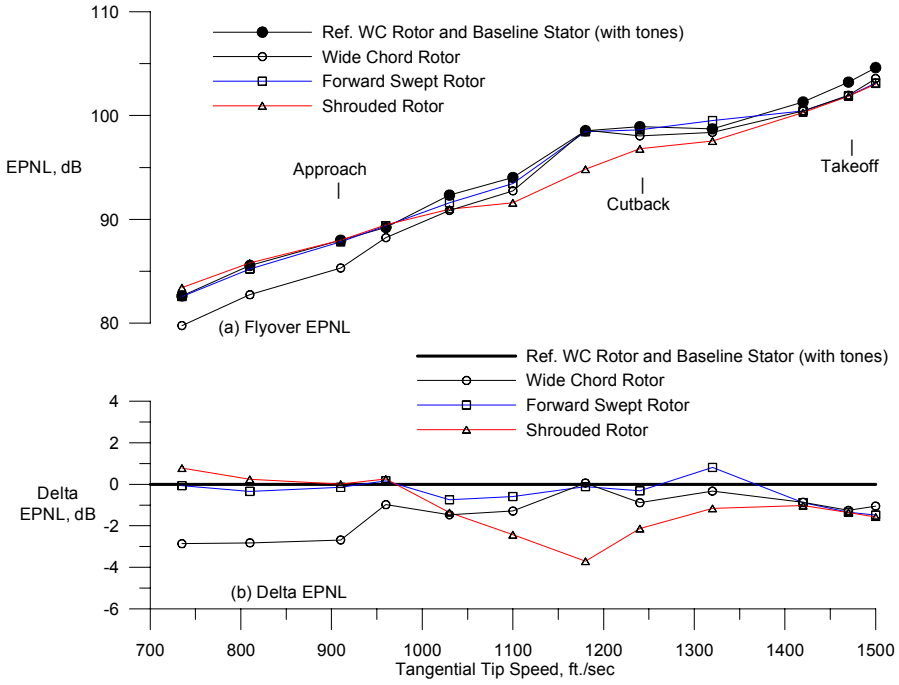

Figure 53.—Flyover EPNL for swept and leaned stator and three rotors with all bypass tones present (core rotor tones removed).

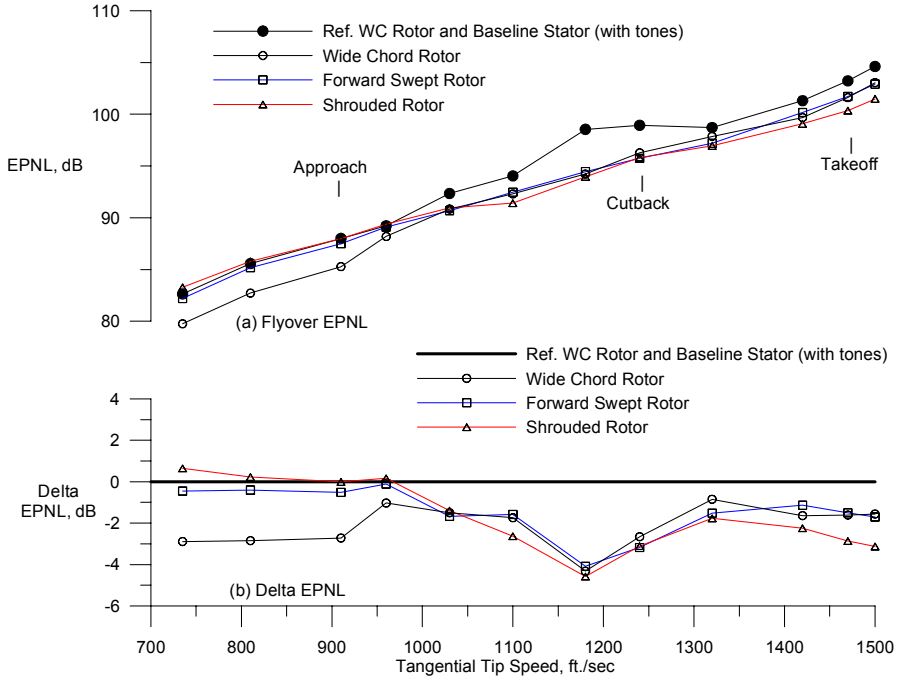

Figure 54.—Flyover EPNL for swept and leaned stator and three rotors with bypass BPF tone removed (core rotor tones removed).

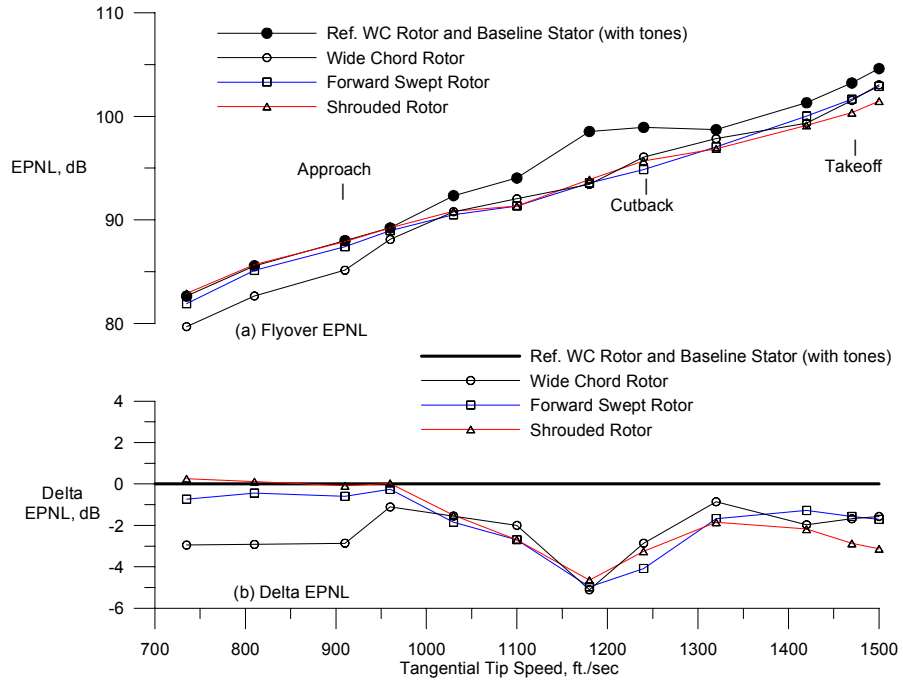

Figure 55.—Flyover EPNL for swept and leaned stator and three rotors with all bypass nBPF tones removed (core rotor tones removed).

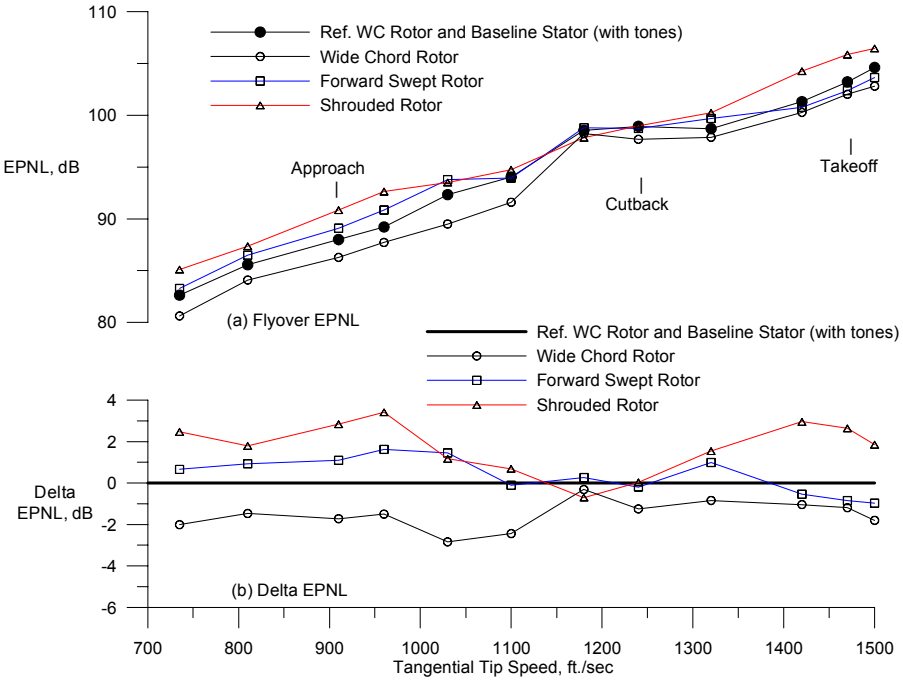

Figure 56.—Flyover EPNL for integral vane/frame stator and three rotors with all bypass tones present (core rotor tones removed).

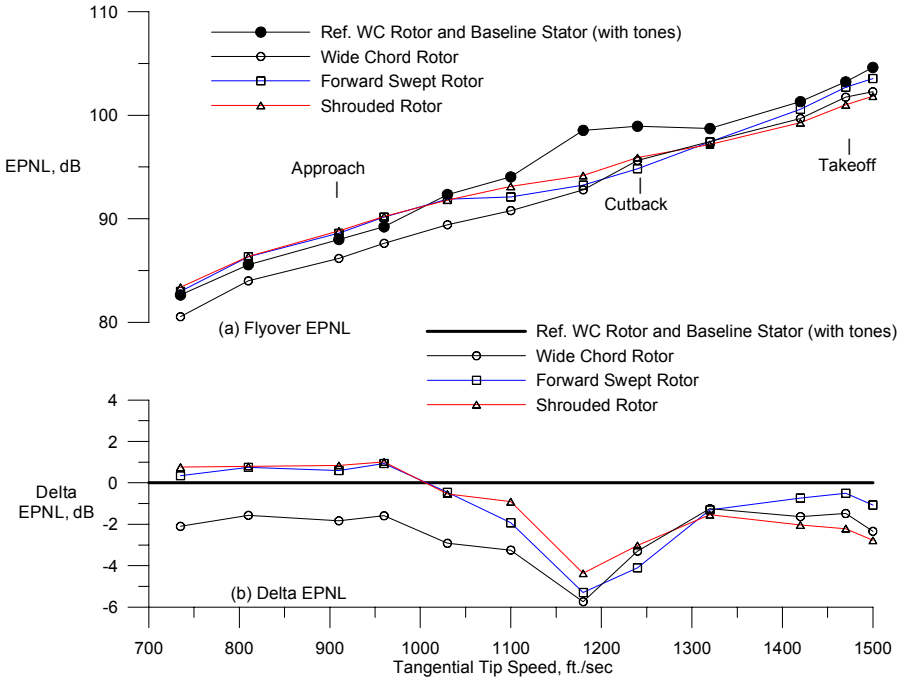

Figure 57.—Flyover EPNL for integral vane/frame stator and three rotors with bypass BPF tone removed (core rotor tones removed).

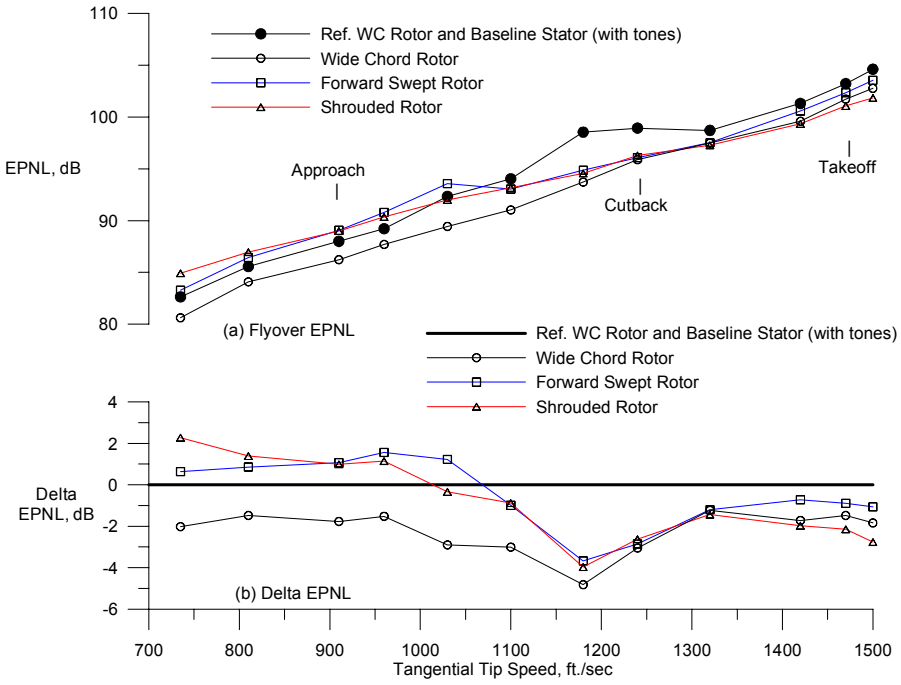

Figure 58.—Flyover EPNL for integral vane/frame stator and three rotors with all bypass nBPF tones removed (core rotor tones removed).

REPORT DOCUMENTATION PAGE

Form Approved
OMB No. 0704-0188

1. AGENCY USE ONLY (*Leave blank*)	2. REPORT DATE	3. REPORT TYPE AND DATES COVERED
	May 2004	Technical Memorandum

4. TITLE AND SUBTITLE

Far-Field Acoustic Characteristics of Multiple Blade-Vane Configurations for a High Tip Speed Fan

5. FUNDING NUMBERS

WBS–22–781–30–08

6. AUTHOR(S)

Richard P. Woodward, John A. Gazzaniga, and Christopher E. Hughes

7. PERFORMING ORGANIZATION NAME(S) AND ADDRESS(ES)

National Aeronautics and Space Administration
John H. Glenn Research Center at Lewis Field
Cleveland, Ohio 44135–3191

8. PERFORMING ORGANIZATION REPORT NUMBER

E–14568

9. SPONSORING/MONITORING AGENCY NAME(S) AND ADDRESS(ES)

National Aeronautics and Space Administration
Washington, DC 20546–0001

10. SPONSORING/MONITORING AGENCY REPORT NUMBER

NASA TM—2004-213093

11. SUPPLEMENTARY NOTES

Richard P. Woodward and Christopher E. Hughes, NASA Glenn Research Center; and John A. Gazzaniga, QSS Group, Inc., 21000 Brookpark Road, Cleveland, Ohio 44135. Responsible person, Richard P. Woodward, organization code 5940, 216–433–3923.

A supplemental CD is included in the back of this report. It contains far-field SPL results for each configuration, EPNL and PWL table, daily acoustic logs, descriptive tables for tests parameters, and technical reports pertaining to the subject fan test. For a complete listing see the file named *CD Contents.pdf* on the supplemental CD.

12a. DISTRIBUTION/AVAILABILITY STATEMENT

Unclassified - Unlimited
Subject Categories: 05 and 07 Distribution: Nonstandard

Available electronically at http://gltrs.grc.nasa.gov

This publication is available from the NASA Center for AeroSpace Information, 301–621–0390.

12b. DISTRIBUTION CODE

13. ABSTRACT ***(Maximum 200 words)***

The acoustic characteristics of a model high-speed fan stage were measured in the NASA Glenn 9- by 15-Foot Low Speed Wind Tunnel at takeoff and approach flight conditions. The fan was designed for a corrected rotor tip speed of 442 m/s (1450 ft/s), and had a powered core, or booster stage, giving the model a nominal bypass ratio of 5. A simulated engine pylon and nozzle bifurcation was contained within the bypass duct. The fan stage consisted of all combinations of 3 possible rotors, and 3 stator vane sets. The 3 rotors were (1) wide chord, (2) forward swept, and (3) shrouded. The 3 stator sets were (1) baseline, moderately swept, (2) swept and leaned, and (3) swept integral vane/frame which incorporated some of the swept and leaned features as well as eliminated the downstream support structure. The baseline configuration is considered to be the wide chord rotor with the radial vane stator. A flyover Effective Perceived Noise Level (EPNL) code was used to generate relative EPNL values for the various configurations. The swept and leaned stator showed a 3 EPNdB reduction at lower fan speeds relative to the baseline stator; while the swept integral vane/frame stator showed lowest noise levels at high fan speeds. The baseline, wide chord rotor was typically the quietest of the three rotors. A tone removal study was performed to assess the acoustic benefits of removing the fundamental rotor interaction tone and its harmonics. Reprocessing the acoustic results with the bypass tone removed had the most impact on reducing fan noise at transonic rotor speeds. Removal of the bypass rotor interaction tones (BPF and nBPF) showed up to a 6 EPNdB noise reduction at transonic rotor speeds relative to noise levels for the baseline (wide chord rotor and radial stator; all tones present) configuration.

14. SUBJECT TERMS	15. NUMBER OF PAGES
Aircraft noise; Jet aircraft noise; Acoustic emission	56
	16. PRICE CODE

17. SECURITY CLASSIFICATION OF REPORT	18. SECURITY CLASSIFICATION OF THIS PAGE	19. SECURITY CLASSIFICATION OF ABSTRACT	20. LIMITATION OF ABSTRACT
Unclassified	Unclassified	Unclassified	